CO_2 INJECTION TO IMPROVE OIL RECOVERY USING ZIPPER HYDRAULIC FRACTURES

by

Goksu Akoglu Somyurek

A thesis submitted to the Faculty and the Board of Trustees of the Colorado School of Mines in partial fulfillment of the requirements for the degree of Master of Science (Petroleum Engineering).

Golden, Colorado

Date _____

Signed: _____

Goksu Akoglu Somyurek

Signed: _____

Dr. Hossein Kazemi

Thesis Advisor

Golden, Colorado

Date _____

Signed: _____

Dr. Erdal Ozkan

Professor and Head

Department of Petroleum Engineering

ABSTRACT

Conventional oil reservoirs are the main source of oil production because they are easier to produce. On the other hand, unconventional reservoirs have considerably lower oil recoveries in spite of their large initial oil in place (IOIP). Despite the innovative technologies of horizontal wells and hydraulic fracturing techniques, the recovery factor for the Bakken, the largest unconventional resource in the United States, is less than 10 percent. The low oil recovery factor from the Bakken resource reveals the need for enhanced oil recovery (EOR). The hydraulic fracture spacing, orientation, and fracture pattern affects the performance of EOR schemes. For instance, a zipper fracture arrangement is believed to improve permeability and create a larger stimulated reservoir volume (SRV) which, in turn, should improve both the primary and EOR recovery factors.

In this thesis, the CO_2 injection-and-soak method was the EOR technique. The CO_2 EOR was modeled using the GEM® (from Computer Modeling Group) compositional reservoir simulator and Bakken reservoir parameters. While keeping reservoir parameters exactly the same, two different hydraulic fracture patterns, a regular pattern and a zipper pattern, were used in the evaluation of both primary production and CO_2 EOR. The primary production was for one year and the CO_2 injection-and-soak method for nine years.

In this study, we did not observe much improvement in oil recovery using the zipper fracture pattern versus a regular fracture pattern. Furthermore, the molecular diffusion effect was insignificant even with values as large as10^{-2} cm^2/s.

TABLE OF CONTENTS

LIST OF FIGURES

LIST OF TABLES

ACKNOWLEDGEMENTS

I thank my advisor, Dr. Hossein Kazemi, who not only enlightened my perspective as a reservoir engineer but also my perspective on life. He always encouraged me, supported me, and inspired me with his wisdom.

I thank my thesis committee members, Dr. Hulya Sarak and Dr. Hazim Abass, for their valuable advice. I am also thankful to all my professors, staff and students in Petroleum Engineering Department at Colorado School of Mines for their support. Most importantly, I acknowledge the Turkish Petroleum Corporation (TPAO) for the M.S. scholarship and funding.

Finally, I thank my father, Mehmet Ali Akoglu, my mother, Gulay Akoglu, and my sister, Seray Akoglu, for their moral support in my whole life. Also my special thanks to my husband, Serdar Somyurek, who stood by my side and brought joy to my life.

CHAPTER 1

INTRODUCTION

According to Energy Information Administration (EIA, 2013), the major unconventional oil reserves are in Russia, United States, China, Argentina, and Libya. While USA is the leader in unconventional oil production. EIA (2013) gives an estimate of 47.7 billion barrels of unconventional reserves for the United States and 14.7 billion barrels for the Bakken.

Production from unconventional reservoirs is relatively new compared to conventional reservoirs. Horizontal wells and multistage hydraulic fracturing are technologies credited for the production from unconventional reservoirs. Nonetheless, the recovery factor from these reserves is around 10 percent. This means that a significant amount of oil is left behind in unconventional reservoirs and enhanced oil recovery (EOR) techniques are needed to recover more oil.

Only one or two conventional reservoir EOR methods, such as CO_2 injection, can possibly be applied in unconventional reservoirs to improve oil recovery. Specifically, CO_2 dissolves in oil rather easily and has a low minimum miscibility pressure (MMP) in unconventional light oils. CO_2 also lowers oil viscosity and swells the oil to enhance oil production (Kurtoglu et al., 2013). Additionally, multi-stage hydraulic fracturing is the flow path to utilize CO_2 and increase oil production; however, fracture morphology, spacing, pattern, and permeability affect the efficiency of the soak and CO_2 injection method. The zipper fracture pattern is one of the advocated geometries (Water et al., 2009, and Warpinski et al., 2009) believed to increase the stimulated reservoir volume (SRV).

1.1 Research Objective

The objective of this research is to evaluate the potential of CO_2 injection for improving oil recovery using the zipper hydraulic fracture pattern in the Bakken. The objectives are two-

fold: First, determining the CO_2 injection applicability in unconventional reservoirs and, second, evaluating the use of zipper-fracture geometry for EOR in unconventional reservoirs.

1.2 Research Methodology

1. Review petroleum geology of the Bakken.
2. Review past and current production of the Bakken.
3. Evaluate CO_2 EOR fundamentals and its potential use in the Bakken.
4. Construct a fully compositional, dual-porosity model for zipper and regular fracture patterns using Bakken crude oil and reservoir parameters.
5. Validate the reservoir model by generating a theoretical multiphase rate transient test and analyze the test to verify the soundness of the reservoir model by correctly recovering reservoir permeability.
6. Compare the oil recovery performance of zipper fracture pattern and regular fracture pattern.

1.3 Organization of the Thesis

Chapter 1 presents the introduction to the research with objectives and methodology.

Chapter 2 presents a literature review. Petroleum geology, production history of the Bakken and need for EOR in unconventional reservoirs are the main topics in this chapter. Water flooding and CO_2 injection EOR will be compared for unconventional reservoirs. The reasons to choose CO_2 injection EOR will be represented.

Chapter 3 is the segment where modeling background is explained. The reservoir rock properties are tabulated. Also, Bakken Crude Oil composition will be presented with compositional model PVT. There are two different types of hydraulic fracture models modeled

for this thesis. One is non-zipper hydraulic fracture and the other is zipper hydraulic fracture. The details of both of the models will be shown in this chapter. Also, model gridding type will be explained.

Chapter 4 presents the results. This chapter starts with rate transient analysis results for validation of the model. Then results for primary production for both non-zipper hydraulic fracture and zipper hydraulic fracture cases are presented. Finally, CO_2 injection application results for different CO_2 injection scenarios are tabulated in this chapter. The comparison for non-zipper hydraulic fracture and the zipper hydraulic fracture for primary production and CO_2 injection are discussed in this segment.

Chapter 5 present conclusions based on the results from Chapter 4.

CHAPTER 2

LITERATURE REVIEW

This chapter starts with petroleum geology of the Bakken, the largest unconventional reservoir in United States. In 2008, the USGS estimated that the mean technically recoverable reserves from the Bakken to be 3.65 billion barrels of oil, 1.85 trillion cubic feet of natural gas, and 148 million barrels of natural gas liquids, which has established Bakken as the largest unconventional resource in the lower 48 states (Pilcher et al., 2011). North Dakota is currently the largest Bakken producer and is the second largest U.S. oil producer behind Texas (DuBose, 2012).

Because the Bakken is a large oil deposit and resource, understanding its geology is critical for those interested in its EOR potential. Similarly, the production history of the Bakken is critical for EOR planning. Because primary production recovery factors are very low, miscible CO_2 injection EOR method is a potential candidate to enhance oil recovery in the Bakken. This will be covered later in this chapter.

2.1 Geology of Bakken

Bakken formation is in the Williston Basin, located in North Dakota, South Dakota, Montana in United States, and Saskatchewan and Manitoba in Canada (Figure 2.1). The Bakken was deposited in Late Devonian to Early Mississippian and consists of Upper, Middle, and Lower Bakken. The Upper and Lower Bakken have similar lithology consisting of organic-rich black shale. The Middle Bakken is fine-grained sandstone and siltstone (Pitman et al., 2001). The Bakken lies between the lower Lodgepole and the upper Three Forks formations (Figure 2.2). While the lower Lodgepole conformably overlays the Bakken, the Three Forks, underlying the Bakken, is conformable in deep parts and less conformable in shallow parts. The thickness of the

Bakken ranges from the wedge edge to more than 140 ft (Figure 2.3). The three components of the petroleum system are lower Lodgepole, three Bakken members, and the upper Three Forks (Sonnenberg and Pramudito, 2009). The Bakken is a typical unconventional reservoir with low permeability and porosity (Theloy and Sonnenberg, 2013).

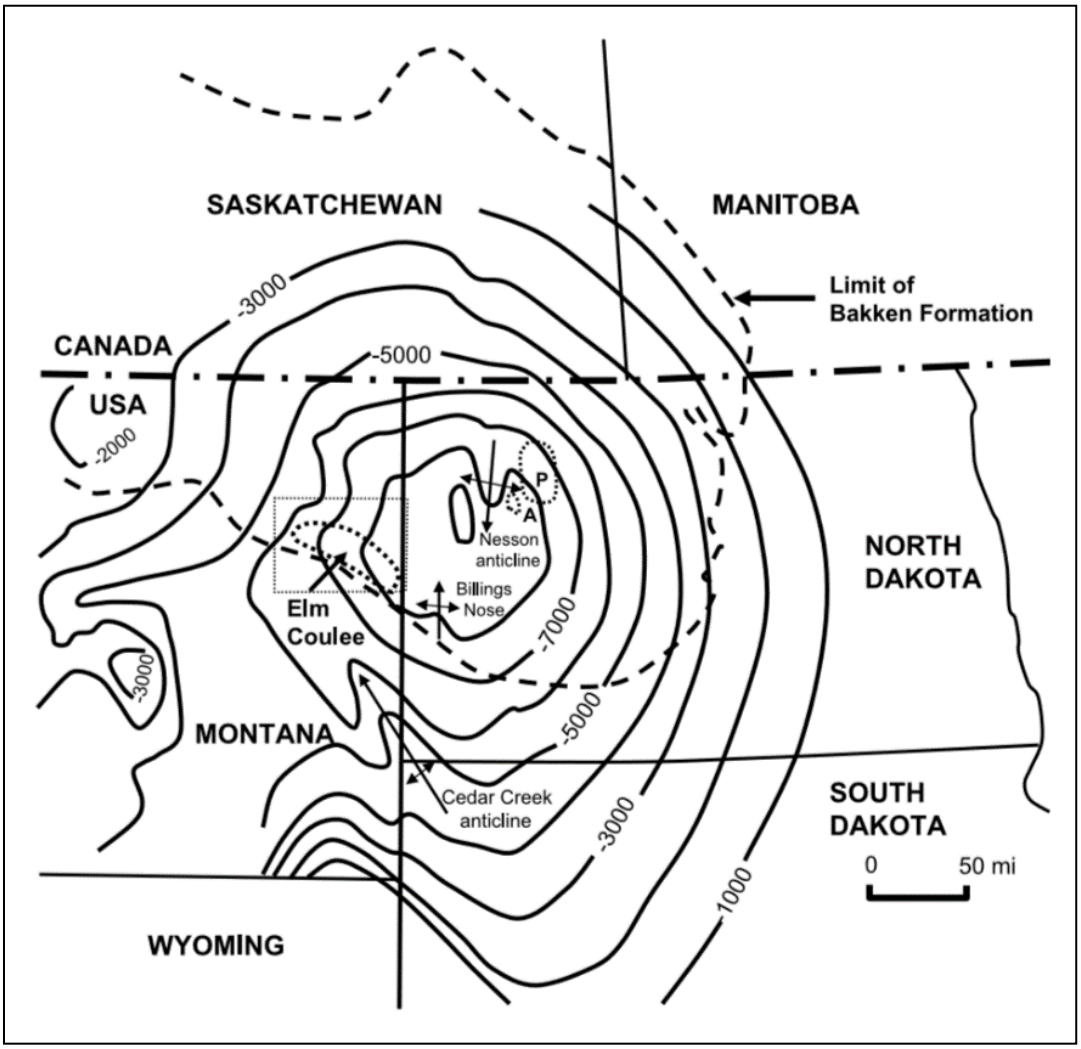

Figure 2.1: Williston Basin Map (Modified from Webster, 1984).

Upper and Lower Bakken are highly organic-rich and constitute the source rock for the Middle Bakken, and are considered the boundaries of the Bakken petroleum system. The quantity of the petroleum generated and produced in the Bakken depends on thickness, thermal maturity and total organic carbon (TOC). The lower member is a dark-gray to brownish-black,

organic-rich shale. The upper member is similar to the lower members, however it has higher TOC - up to 36 weight percent (Pitman et al., 2001).

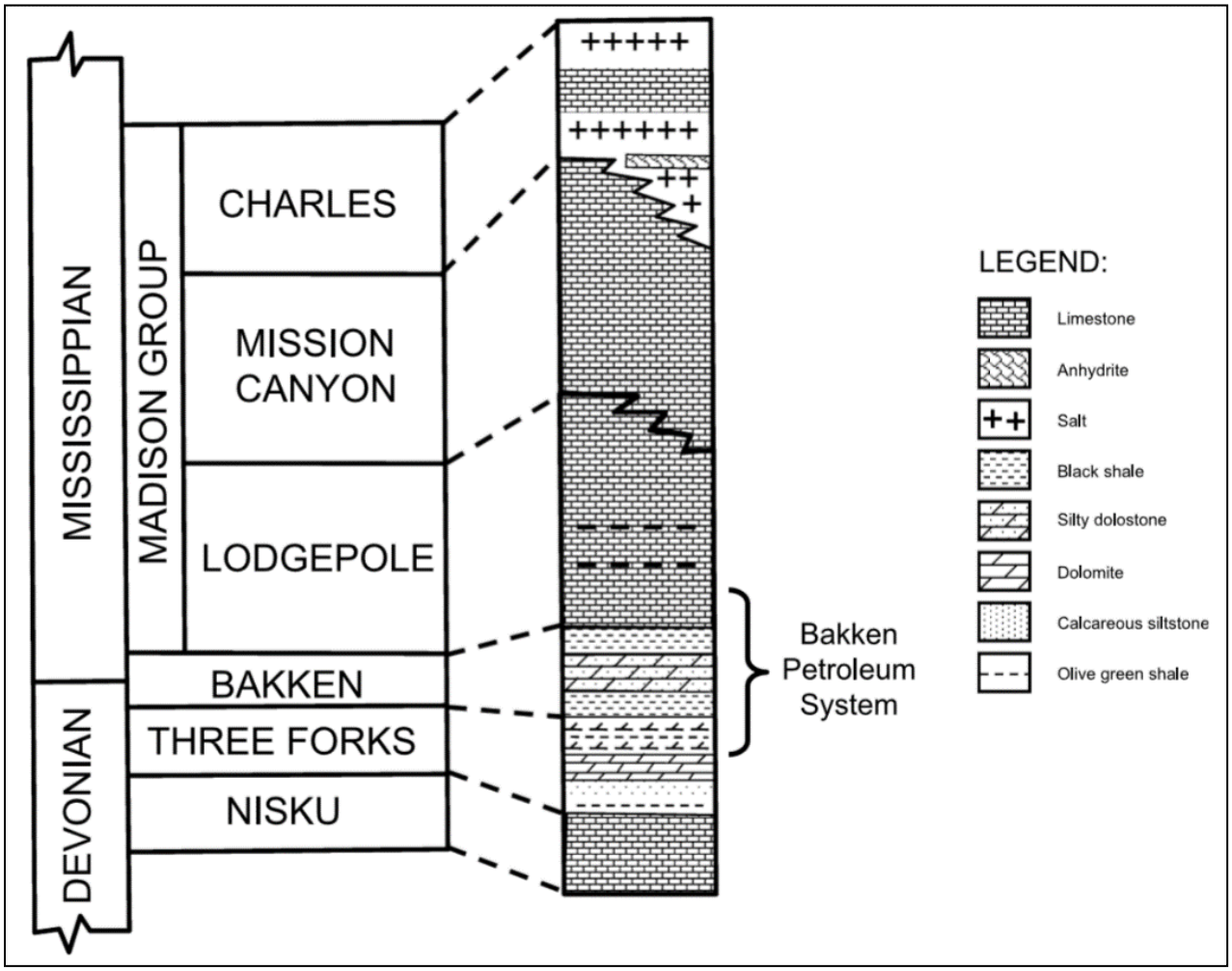

Figure 2.2: Bakken Lithology (Modified from Webster, 1984).

The Middle Bakken lithology is complex and consists of sandstone, limestone and siltstones (Pitman et al., 2001). The main oil production target is dolomitic siltstone to silty dolomite in the Middle Bakken and upper Three Forks (Theloy and Sonnenberg, 2013). The Middle Bakken depth is from 8,500 to 10,500 feet, its thickness from 8 to 14 feet (Sonnenberg and Pramudito, 2009), average porosity 5%, average permeability 0.04 md (Pitman et al., 2001) and TOC ranging around 0.1 to 0.3 percent by weight (Price, 1999).

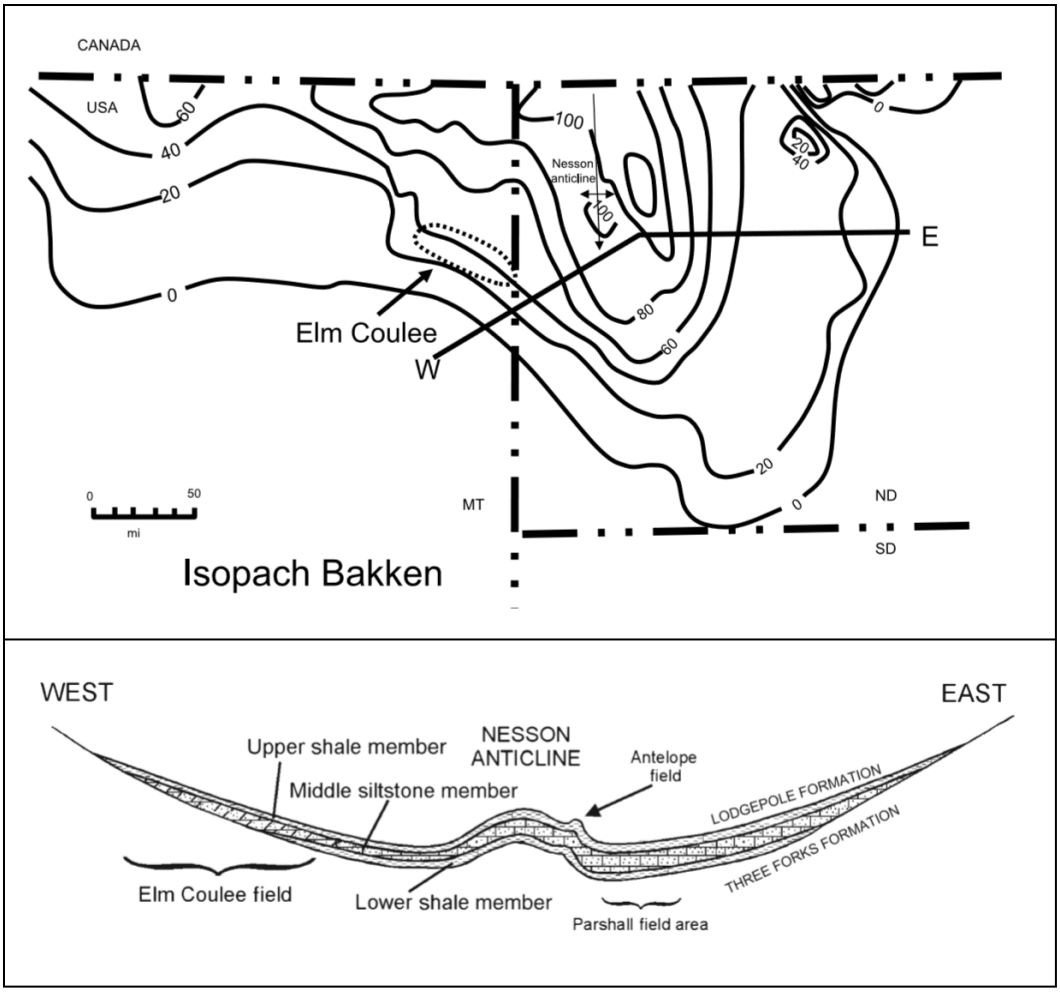

Figure 2.3: Schematic Cross Section of Bakken (Modified from Meisner, 1978).

2.2 Production History

The production from Bakken and Three Forks started in 1953 with the discovery of Antelope field. Initial wells drilled were vertical. In 1987, the first horizontal well was drilled and after that horizontal wells dominated production from Bakken (LeFever and LeFever, 2005). In early 1990s hydraulic fracturing was applied in horizontal wells. In early 2000 companies utilized multistage hydraulic fractures which increased production (Sonnenberg and Pramudito, 2009). Ever since, horizontal well and hydraulic fracturing became the key factors for economic oil production in the Bakken. In the year 2000, North Dakota's total oil production was less than 2,000 barrels per day (bbl/d) while the producing well number was around 200. By 2014, the

total oil production exceeded 1,000,000 bbl/d and the producing well number was 8,500 (Figure 2.4 and Figure 2.5) (NDIC, 2015).

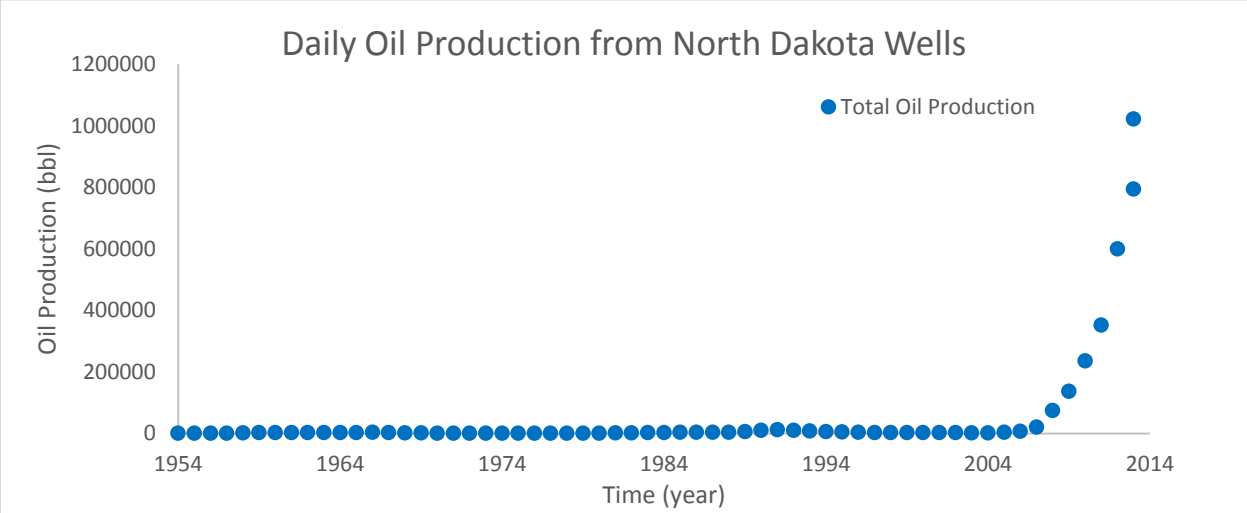

Figure 2.4: Average Daily Oil Production from North Dakota Wells (NDIC, 2015).

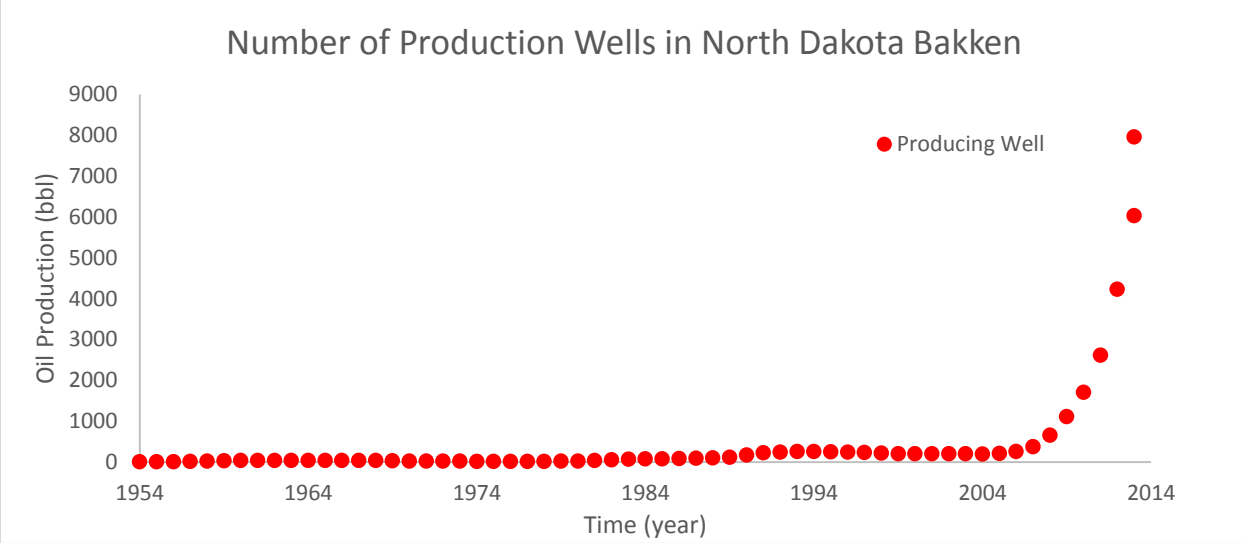

Figure 2.5: Average Number of Wells in Production from North Dakota (NDIC, 2015)

2.3 EOR Potential of Bakken

USGS has reported recoverable oil estimate of 7.4 billion barrels of oil, 6.7 trillion cubic feet of natural gas, and 0.53 billion barrels of natural gas liquids (NGL) from Bakken and Three Forks (Gaswirth et al., 2013). Unfortunately, the oil recovery factor translates to less than 10

percent of the oil in place. To increase recovery factor, an EOR method must be devised. The reservoir has very low matrix permeability, which we believe will result in unsuccessful water flooding. Although water flooding is the most common recovery technique after primary production in conventional reservoirs, it is not the case in low-permeability reservoirs. Less viscous CO_2 would be the best option to enhance oil recovery from Bakken with higher injectivity. CO_2 and oil are multi-contact miscibility which means the mass transfer between oil and CO_2 will continue until these two fluids cannot be distinguished from each other. While they are mixing, CO_2 condenses into oil and lighter components of oil vaporize into CO_2. This make the oil more mobile (Jarrell et al., 2002). CO_2 can only be dissolved in oil above a specific pressure called minimum miscibility pressure (MMP). The key to designing a proper CO_2 injection is to reach multi-contact miscibility which will reduce viscosity and end up with oil swelling (Wang et al., 2010). Even though CO_2 injection is in the research phase, there are some promising results in the literature. For example Shoaib and Hoffman (2009) claim that the recovery increases 20% with CO_2 injection for the Elm Coulee field which is a part of the Bakken.

In this research CO_2 injection is applied for both zipper hydraulic fracturing cases and non-zipper hydraulic fracturing cases. In both cases, there are two identical wells. One of those wells will turn into an injection well after one year of depletion. Different scenarios will be applied for CO_2 injection cases for both models.

CHAPTER 3

NUMERIC MODEL

In this study, the GEM® (Computer Modelling Group) dual-porosity, fully compositional model was used to simulate primary depletion and CO_2 EOR. This software was chosen because the simulator is capable of providing results for a variety of engineering applications such as project development and economic analysis. This chapter includes model description, reservoir volume and well locations, gridding, hydraulic fracture orientation, reservoir rock properties with relative permeability curves, and reservoir fluid properties with PVT analysis.

3.1 Model Description

The model used a dual-porosity, fully compositional model with nine components. Detailed analysis of the fluid composition is presented in the PVT section. The advantage of using a fully compositional model is that it captures the mass transfer between vapor and liquid phases more accurately. However, it makes the run times longer. The model is dual-porosity because field data suggest that the unconventional reservoirs are naturally fractured reservoirs which can be modeled better by dual-porosity. In the dual-porosity model, the flow hierarchy is from matrix to micro-fractures, to macro-fracture network, to multi-stage hydraulic fractures, and, finally, to the horizontal well bore (Kurtoglu, 2013).

To observe the effect of zipper fracture geometry versus non-zipper fracture geometry, two different models were built. In both cases, the reservoir volume, well distance and number of hydraulic fracture and parameters (length, conductivity) are assumed equal.

The model assumptions are:

- Nine components: CO_2, C1, C2, C3, C4, C5-C6, C7-C12, C13-C21, C22-C80.

- Peng-Robinson Equation of State (EOS).
- The matrix and fracture, three-phase relative permeability curves are that of Stone's second equation (Stone, 1973).
- Capillary pressures effects are neglected.
- The dual-porosity shape factor for is that of Kazemi et al. (Kazemi et al., 1976).
- The reservoir is isothermal.

A reservoir segment was modeled with a logarithmic gridding in the x-direction only. In the y-direction and z-direction, uniform gridding was used.

Hydraulic fractures in the y-direction were assigned at smallest grid in x-direction.

With the above assumptions, only a segment of the reservoir was modelled assuming symmetry in the entire system. In each segment, there are two wells which are parallel to each other with same parameters. The difference between a zipper fracture and a non-zipper fracture is the hydraulic fracture location (Fig. 3.1 and Fig. 3.2).

3.1.1 Reservoir Volume and Well Locations

In this research the base shape of the reservoir is rectangular. For both hydraulic fracture cases, the reservoir volume is assumed equal. To apply symmetry, only the well location of the middle well was changed to create a zipper hydraulic fracture from the base reservoir. In the schema of the reservoirs, there are three horizontal wells in both cases which have equal length and number of hydraulic fractures with same parameters and the only difference is the distribution of hydraulic fractures. For non-zipper hydraulic fracture case, there are 10 stages of

hydraulic fractures for each well, and the hydraulic fracture tips are collinear. On the other hand, there are 10 stages of hydraulic fractures for each well for the zipper hydraulic fracture case and these fractures are in-between the two hydraulic fractures of the other well. Total well length is 4300 ft and thickness of the model is 50 ft. The distance between the wells is 650 ft and the hydraulic fracture half-length is 122.5 ft. The reservoir boundaries are 325 ft away from top and bottom boundaries and 215 ft away from left and right boundaries. Figure 3.1 and Figure 3.2 show the fracture configuration for zipper hydraulic fractures and non-zipper hydraulic fractures for same reservoir area.

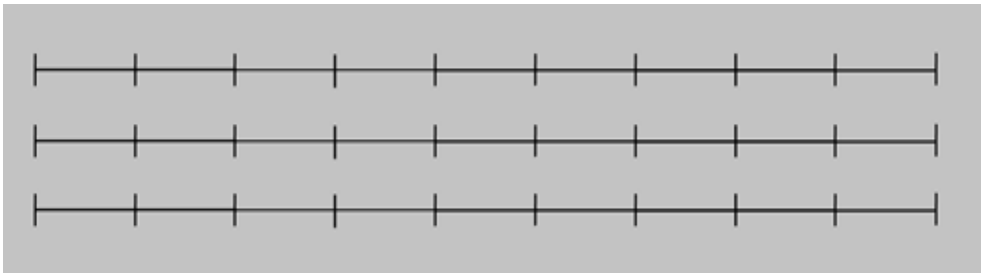

Figure 3.1: Non-Zipper Hydraulic Fracture Configuration.

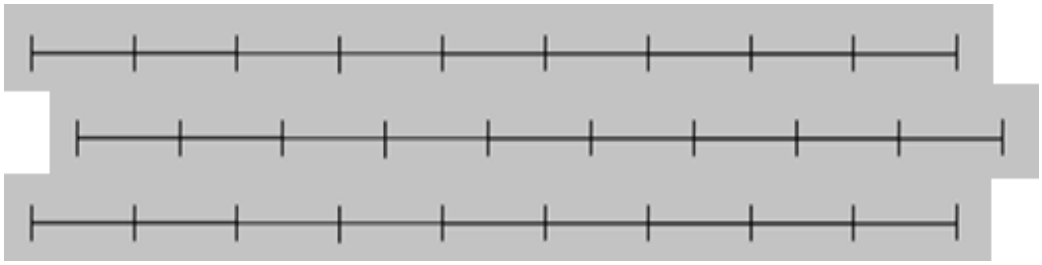

Figure 3.2: Zipper Hydraulic Fracture Configuration.

The goal for making the zipper hydraulic fractures instead of non-zipper hydraulic fractures is to increase the stimulated reservoir volume (SRV). For unconventional reservoirs, which means the matrix permeability is very low, creating complex network between hydraulic fractures and natural fractures with successful treatment is the key factor for commercial production (Rafiee et al., 2014). Since zipper fracture treatment provides better reservoir

interaction with enlarged SRV, zipper fractures are proposed to be a better fracture treatment than non-zipper fracture treatment. In this research the effect of zipper hydraulic fracture versus non-zipper hydraulic fracture will be investigated for both primary production and CO_2 injection.

3.1.2 Gridding for the Model

For this research, logarithmic grid refinement is used due to it giving better understanding around the smaller size grids (Kazemi et al., 1978). Smaller grid sizes are placed around the hydraulic fracture because when production takes place the flow will occur through these hydraulic fractures from the reservoir. Also, when CO_2 injection starts, again the CO_2 will pass through hydraulic fracture to the reservoir. That's why the grid of the model is chosen as logarithmic for only x axis. For y-direction and z-direction uniform grids are used and the system is divided into equal layers. To save on long run times, segments of the reservoir are modeled using GEM® (CMG). Since all of the properties will remain the same, the segment is linearly representing the reservoir.

First, model is validated by rate transient analysis. To apply rate transient analysis, a specific segment of the reservoir is modeled. In this specific segment, the fracture length is set to be equal to the reservoir segments boundary. Only 215 ft of the well segment is modeled. Total length of each well was 4300 ft. which means 1/20 portion of the well is representative. By multiplying the production of that portion by 20, the total production of the well can be found. LRG is used for only the x-direction. Hydraulic fracture is set to be at the smallest grid block in x-direction in order to be able to capture better production and injection data. Total number of logarithmic grids in x-direction is 31. The uniform grid number for y-direction is 13 and z-direction is 5. The hydraulic fracture is at the 16^{th} grid block where the grid is the smallest in x-direction (Figure 3.2).

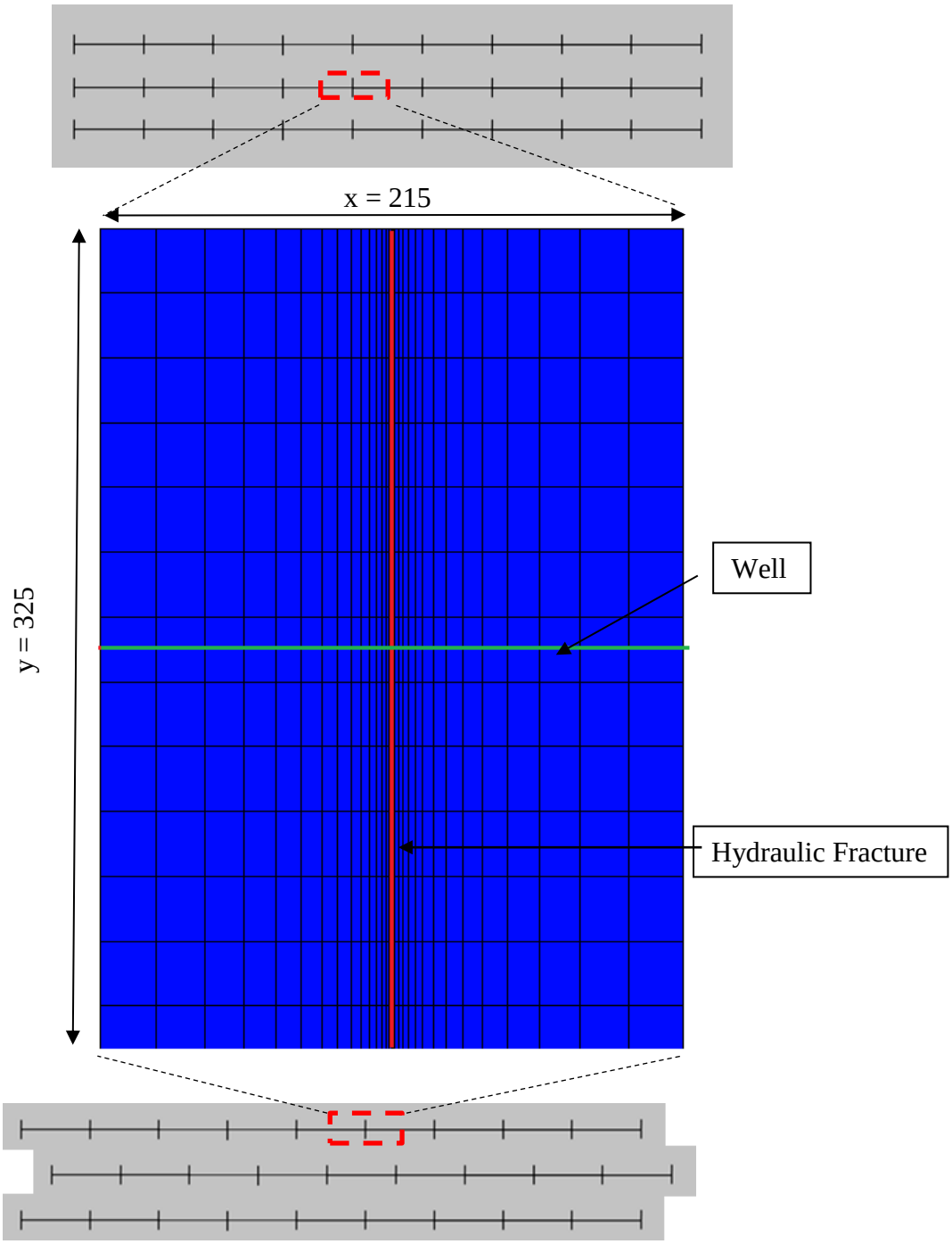

Figure 3.3: Flow Analysis Reservoir Segment.

To make comparison between non-zipper and zipper hydraulic fractures, first both cases are depleted by primary production. For both cases, a 215 ft long portion of the reservoir is modeled. Again logarithmic grid refinement is used for x-axis. Total number of grids in x-

direction will change for the two cases. For zipper hydraulic fracturing case the reservoir is divides into 37 logarithmic grid blocks in x-direction, 13 and 5 uniform grid blocks in y-direction and z-direction respectively. The hydraulic fractures are set to be at the 1st, and the 37th grid blocks (Figure 3.4).

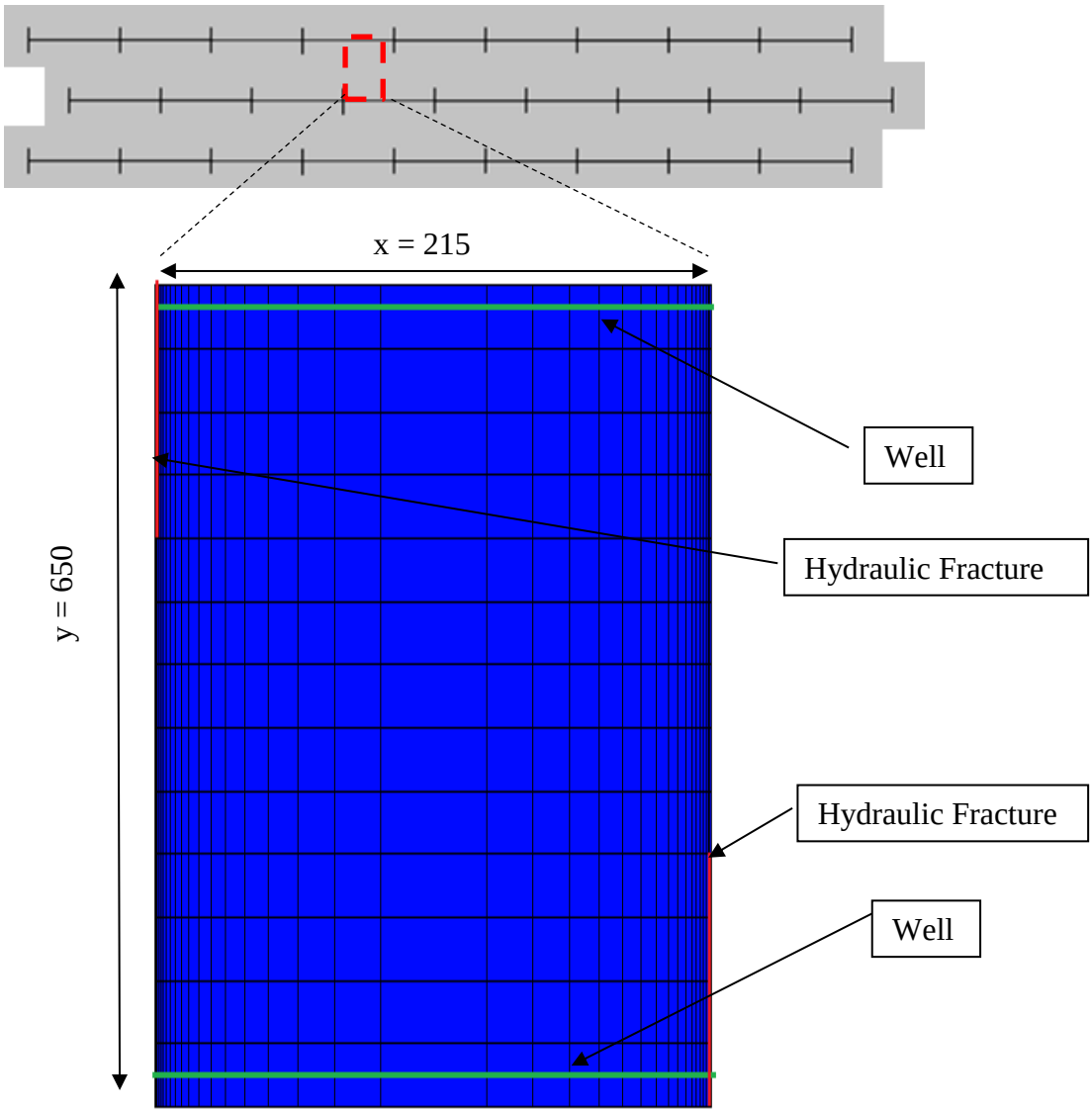

Figure 3.4: Zipper Hydraulic Fracture Case Reservoir Segment.

For non-zipper hydraulic fracturing case the reservoir is divided into 21 logarithmic grid blocks in x-direction, and the rest is the same as the zipper hydraulic fracture case. The hydraulic fracture is in the 1st grid block (Figure 3.4).

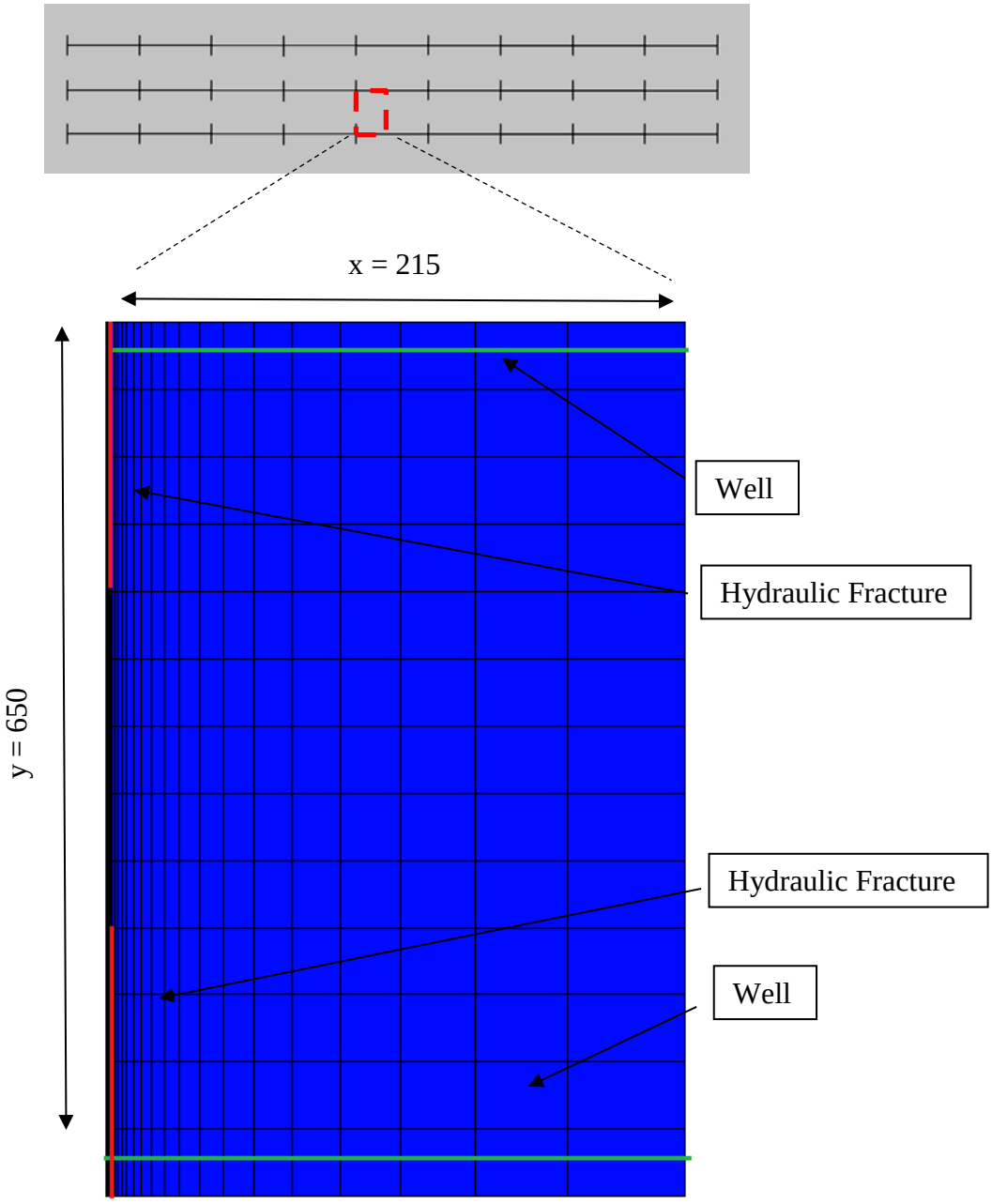

Figure 3.5: Non-Zipper Hydraulic Fracture Case Reservoir Segment

After analyzing the performances of the two different hydraulic fracture configurations for primary depletion, CO_2 injection started. The same reservoir segments are used to compare the results. For CO_2 injection runs, one of the wells will be turned into injection, and the other

will continue production. Different scenarios will be run to analyze the hydraulic fracture configuration effects.

3.2 Reservoir Properties

In this research properties of the Middle Bakken member of the Bakken petroleum system are used. The reservoir properties, hydraulic fracture properties and initial conditions used in this research are tabulated below (Table 3.1, Table 3.2 and Table 3.3) (Kurtoglu and Kazemi, 2012).

Table 3.1: Reservoir properties

Reservoir Properties	
Thickness (ft)	50
Horizontal Well Length (ft)	4300
Reservoir Segment Length (ft) (x-direction)	215
Hydraulic Fracture length (ft)	122.5
Initial Pressure (psia)	6500
Initial Temperature (℉)	241

Table 3.2: Reservoir properties of Middle Bakken (Kurtoglu and Kazemi, 2012)

Reservoir Properties	
Matrix Permeability (md)	1E-05
Natural Fracture Permeability (md)	0.011
Matrix Porosity (fraction)	0.05
Natural Fracture Porosity (fraction)	0.0024
Rock Compressibility (1/psia)	1E-05
Natural Fracture Compressibility (1/psia)	1E-06

Table 3.3: Hydraulic Fracture (Kurtoglu and Kazemi, 2012)

Hydraulic Fracture Properties	
Width (ft)	2
Permeability (md)	50

3.2.1 Reservoir Rock Properties

In this study the flow is considered as three phase flow. The relative permeability curves for this three phase flow are generated for both matrix and fracture. Table 3.4 shows the data used to generate the plots (Kurtoglu and Kazemi, 2012).

Table 3.4: Relative Permeability Data (Kurtoglu and Kazemi, 2012)

Matrix Relative Permeability				Fracture Relative Permeability			
Water-Oil System		Gas-Oil System		Water-Oil System		Gas-Oil System	
k_{rw}*	0.024	k_{rg}*	0.096	k_{rw}*	0.4	k_{rg}*	0.5
k_{row}*	0.103	k_{rog}*	0.103	k_{row}*	0.8	k_{rog}*	0.8
S_{wr}	0.531	S_{lq}	0.73	S_{wr}	0.05	S_{lq}	0.1
S_{orw}	0.211	S_{gr}	0	S_{orw}	0.05	S_{gr}	0
n_w	1.5	n_g	2	n_w	1.5	n_g	2
n_{ow}	2.5	n_{og}	2.5	n_{ow}	2	n_{og}	2

The Stone's second three phase oil relative permeability model was used (Stone, 1973). The equations that used to generate this model, Equations 4.1 to 4.4, are listed below.

For water-oil system:

$$k_{rw} = k_{rw}^{*}\left(\frac{S_w - S_{wr}}{1 - S_{orw} - S_{wr}}\right)^{nw} \quad [3.1]$$

$$k_{row} = k_{row}^{*}\left(\frac{S_o - S_{or}}{1 - S_{orw} - S_{wr}}\right)^{now} \quad [3.2]$$

For liquid-gas system:

$$k_{rg} = k_{rg}^{*}\left(\frac{S_g - S_{gr}}{1 - S_{lg} - S_{gr}}\right)^{ng} \quad [3.3]$$

$$k_{rog} = k_{rog}^{*}\left(\frac{S_l - S_{lg}}{1 - S_{lrg} - S_{gr}}\right)^{nog} \quad [3.4]$$

The relative permeability curves are plotted and shown in Figure 3.6.

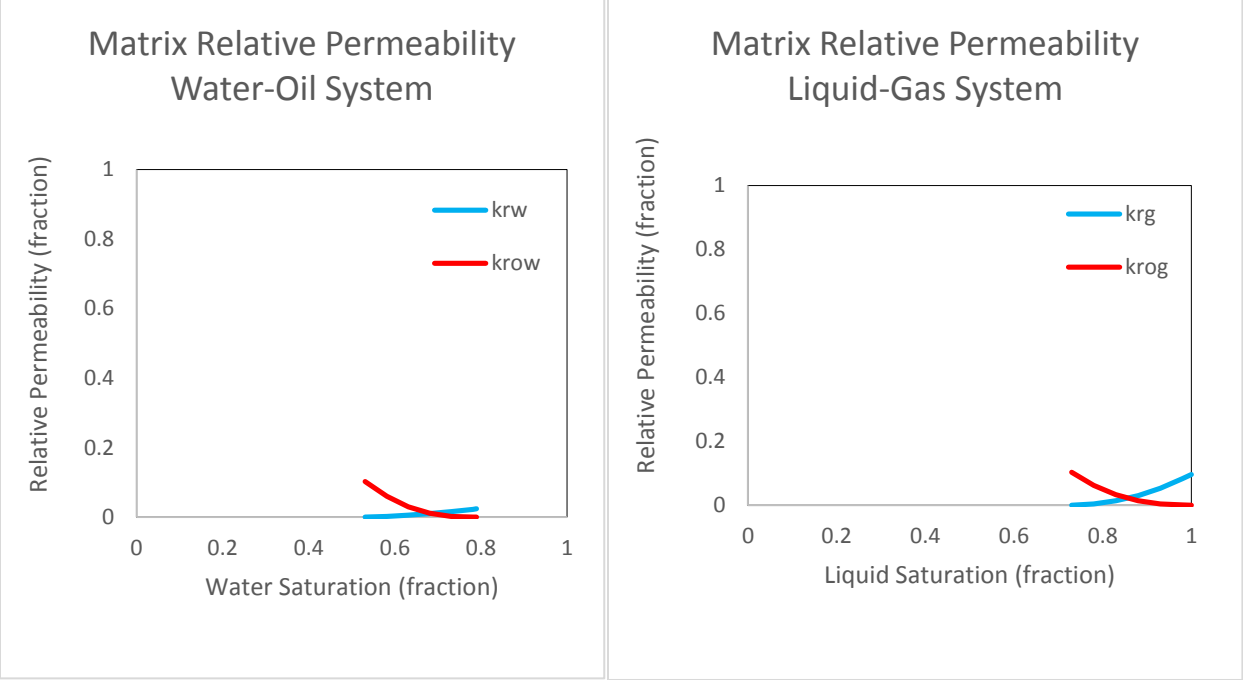

Figure 3.6: Matrix Relative Permeability for Water-Oil System and Liquid-Gas System.

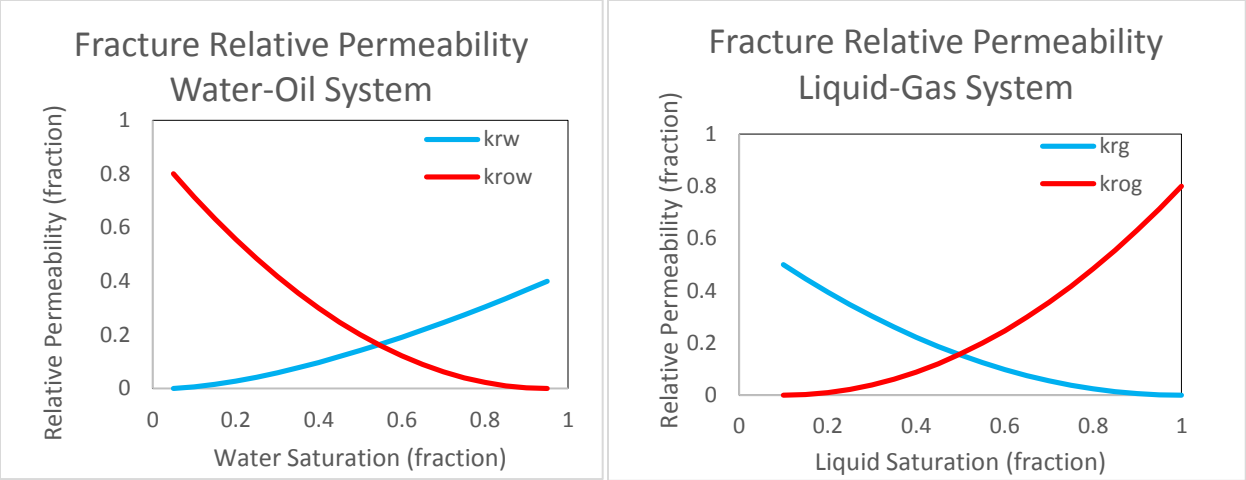

Figure 3.7: Fracture Relative Permeability for Water-Oil System and Liquid-Gas System.

3.2.2 Reservoir Fluid Properties

3.2.2.1 Bakken Crude Oil Composition

In this thesis Bakken crude oil composition is used to run the compositional model which is tabulated in Table 3.5 (Teklu et al., 2014).

Table 3.5: Bakken Crude Oil Composition (Teklu et al., 2014)

Bakken Crude Oil Composition Equation of State (EOS) Peng-Robinson	
CO_2	0.0
C1	36.74
C2	14.89
C3	9.33
C4	5.75
C5-6	6.41
C7-12	15.85
C13-21	7.33
C22-80	3.70
Total	100.0

3.2.2.2 PVT Analysis

By using the composition provided and PVT tool WINPROP® (CMG) the two phase boundary line is created (Figure 3.7). The two phase boundary line is represented with the blue line and the critical point with the red dot, calculated as 3763.66 psia and 592.15°F from WINPROP® (CMG). The initial pressure is 6500 psia and initial temperature is 241°F which is above the two phase line on the left side of the graph. This indicates that the reservoir fluid is a black oil system.

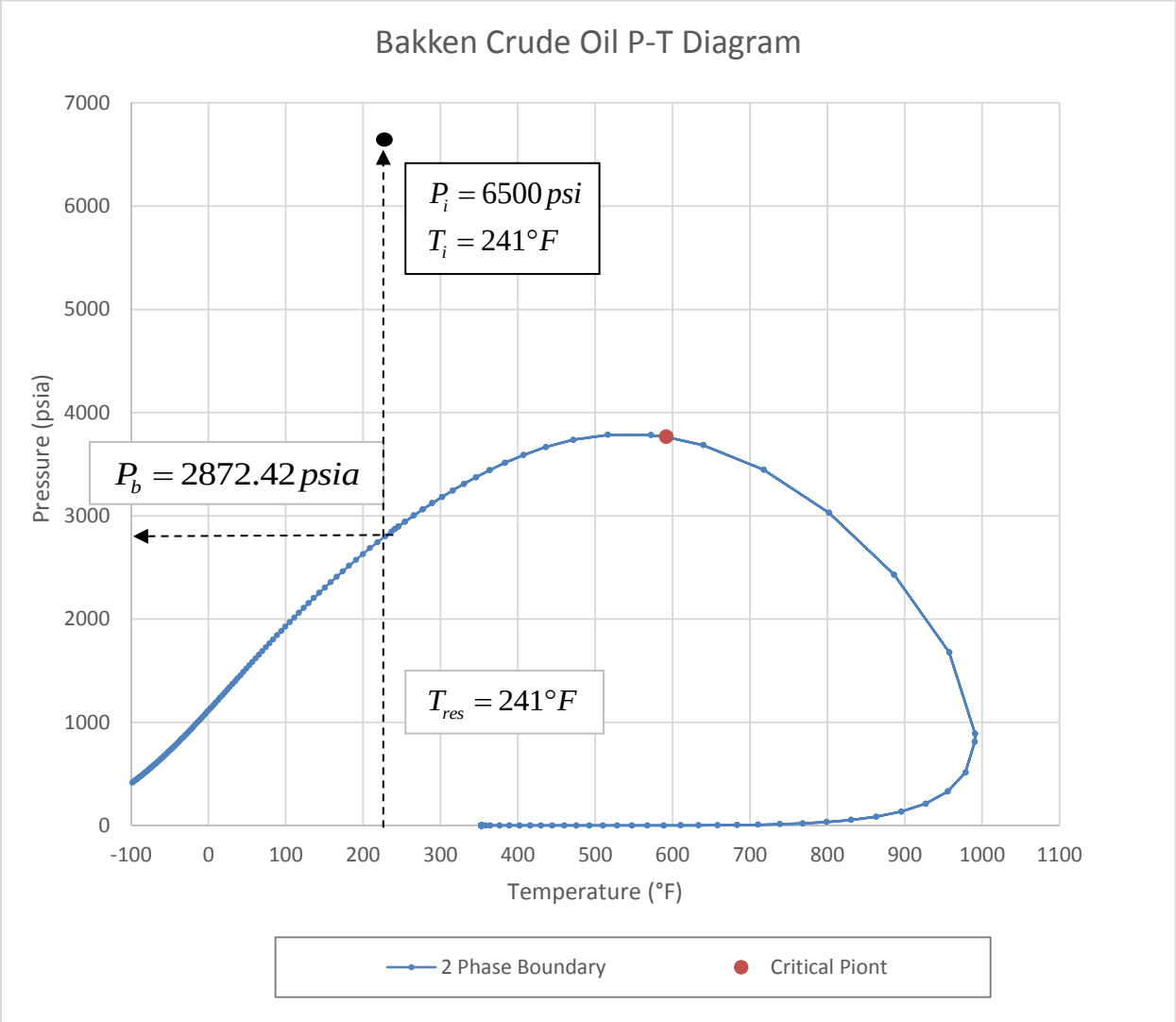

Figure 3.8: Bakken Crude Oil P-T Diagram.

In black oil systems if the two phase boundary has not been reached, in other words above bubble point, the fluid is composed of oil and dissolved gas which means the only phase is liquid. When pressure drops below bubble point pressure the dissolved gases release from the oil and become free gas. This means produced gas at the surface comes from both free gas and dissolved gas.

In this study the model is built as an isothermal model, which means the temperature of the system will remain constant during production and injection. With this condition the bubble point pressure from two phase diagram can be determined. The pressure crossing the two phase diagram at 241°F (initial temperature) is 2872.42 psia which is the initial bubble point pressure for this composition.

3.3 Methodology

1. Deplete the reservoir by primary production.
2. Evaluate the performance of the model using $\frac{\Delta P}{\Sigma qB}$ vs $\sqrt{t}$ and diagnostic plots.
3. Inject CO_2 into the reservoir via zipper fractures to determine the effectiveness of zipper type hydraulic fractures.
4. Compare the results.

CHAPTER 4

RESULTS

This chapter starts with the validation of the model. The model was the GEM® (Computer Modelling Group). A specific segment was modeled to run the production test. After validating the model, primary depletion runs were made to compare zipper hydraulic fracture and non- zipper hydraulic fracture performances. This comparison was extended to CO_2 injection. Different scenarios were tested to develop a better understating on hydraulic fracture performance.

4.1 Multiphase Rate Transient Analysis

To analyze the production data, multiphase rate transient analysis method is used. Particularly, linear flow model is used for a specific reservoir segment. For linear flow model reservoir segment is specifically designed to capture the effects of the mathematical model more accurate. This analytical approach gives better results if the hydraulic fractures are reaching the boundaries of the reservoir so the reservoir boundary length is design to be equal to hydraulic fracture half-length for this specific segment is designed for this case (Chapter 3).

Multiphase rate transient analysis uses rate normalized pressure vs. square root of time. Rate normalized means pressure drop divided by total reservoir flow at reservoir conditions. This model assumes that the main oil is in the reservoir matrix where the oil flows into micro-fractures in the system locally with time. This oil linearly goes through micro-fractures to hydraulic fractures, and oil is produced from horizontal wells through hydraulic fractures. This assumption does not count on the unstimulated region.

To analyze the segment, one year production for the segment of the reservoir which has only one hydraulic fracture is run with constant bottom whole pressures with 3000 psia. Log-log diagnostic plot is drawn in order to determine flow regimes (Figure 4.1).

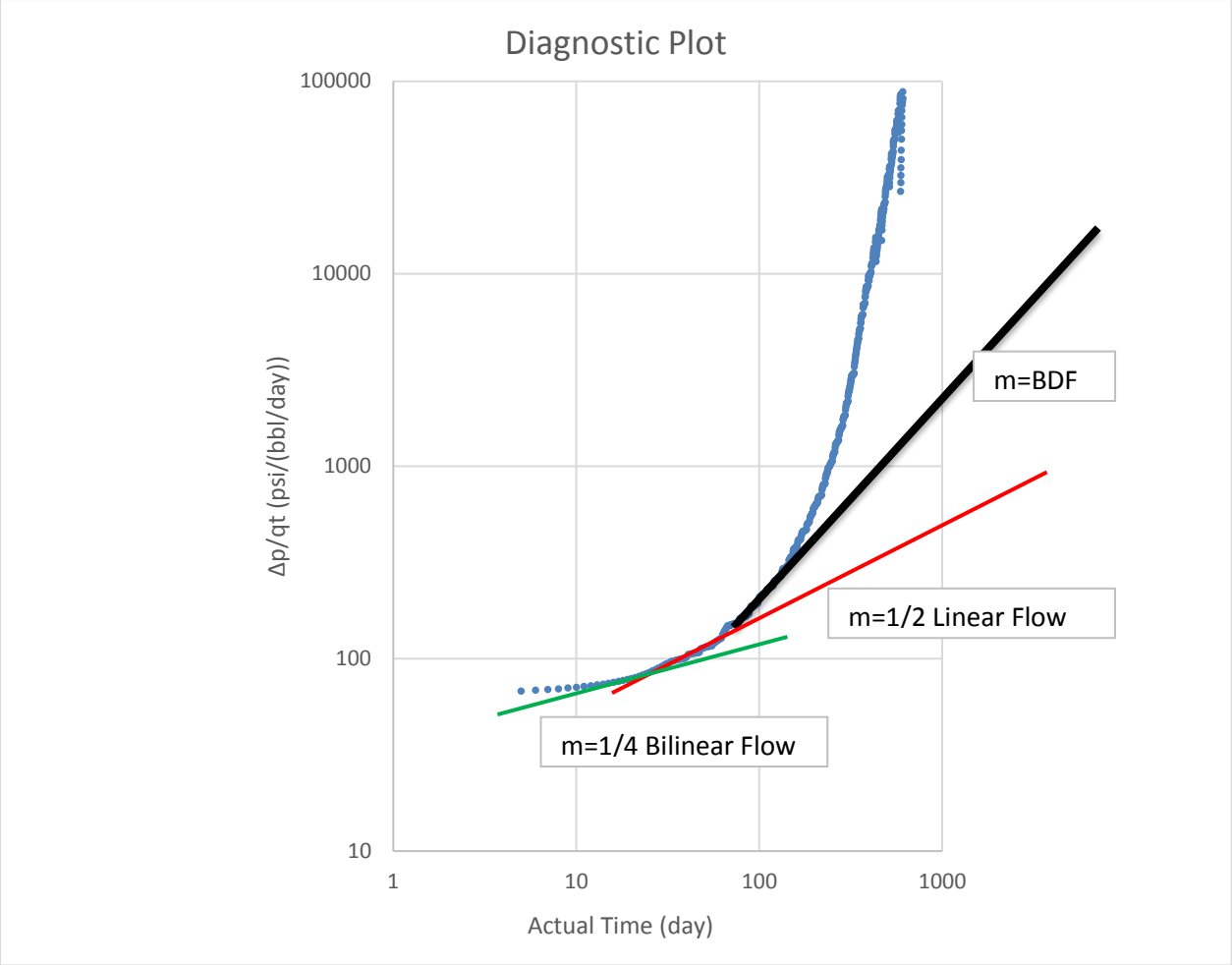

Figure 4.1: Diagnostic Plot.

From the diagnostic plot for one year production for one hydraulic fracture model, since this is an ideal model, three different flow regimes are observed. The flow starts with bilinear flow with slope of 1/4. This flow is a combination of two linear flows. One is from micro-fractures to hydraulic fractures and the other is from hydraulic fractures to the well. After bilinear flow, linear flow takes place with slope of 1/2. In linear flow there is only one flow to

the well which is coming from the stimulated reservoir volume. Finally boundary-dominated flow (BDF) follows with the slope of one occurs. When boundary-dominated flow begins this means that the stimulate reservoir volume is drained without the contribution of unstimulated region.

The equation below is the solution of multiphase fluid diffusivity equation for the infinite acting period (Eker et al., 2014).

$$\frac{\Delta p_{wf}}{q_{total}} = \frac{4.064\sqrt{24}\left(\pi/2\right)\lambda_t}{\sqrt{k_{f,eff}}\left(hn_{hf}\,y_{hf}\right)}\left[\left(\frac{\lambda_t}{\left(\phi c_t\right)_{f+m}}\right)^{1/2}\right]\sqrt{t} + \frac{141.2\lambda_t^{-1}}{k_{f,eff}\,hn_{hf}}\,s_{hf}^{face} \qquad [4.1]$$

For this study, multiphase linear flow analysis is used. The slope of linear flow time period on $\frac{\Delta p_{wf}}{q_{total}}$ vs. $t^{1/2}$ graph is used to recalculate $k_{f,eff}$ (Figure 4.2).

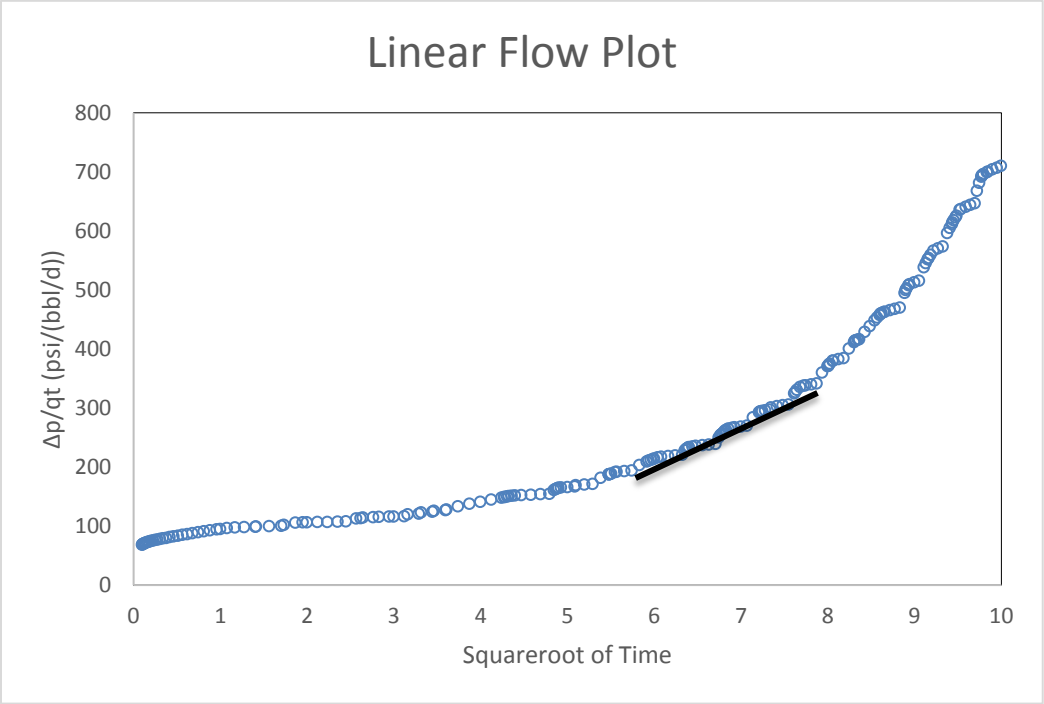

Figure 4.2: Linear Flow Rate Transient Analysis.

Here the slope from $\frac{\Delta p_{wf}}{q_{total}}$ vs. $t^{1/2}$ plot which will refer as m_l is obtained by linear flow period. The linear flow time period is found from the diagnostic plot as 33 to 76 days. Then it is used to recalculate $k_{f,eff}$ with the Equation 4.2 by ignoring the second term since skin is taken as zero (Eker et al., 2014).

$$m_l = \frac{4.064\sqrt{24}\left(\pi/2\right)\lambda_t}{\sqrt{k_{f,eff}}\left(hn_{hf}\,y_{hf}\right)}\left[\left(\frac{\lambda_t}{\left(\phi c_t\right)_{f+m}}\right)^{1/2}\right] \qquad [4.2]$$

The $k_{f,eff}$ value which was entered into the model was 0.011 md and the calculated is 0.0116 md. With this calculation the model is validated.

Table 4.1: Effective Permeability

$k_{f,eff}$	
Model	0.011 md
Calculated	0.0116 md

4.2 Depletion by Primary Production

After validating the model, to compare zipper and non-zipper hydraulic fracture cases, the reservoir is depleted by primary production. Both zipper and non-zipper hydraulic fracture cases have two identical producer wells (Chapter 3) which are producing with constant bottom hole pressures with 2000 psia. The results are shown in Figure 4.3 and Figure 4.4.

From the oil production graph, the produced oil data versus time are identical for both wells in zipper and non-zipper hydraulic fracture configurations. Since the well parameters are

identical, production data are expected to be same. Also for the same reservoir volumes and same well parameters the zipper and non-zipper hydraulic fracture cases give identical production data.

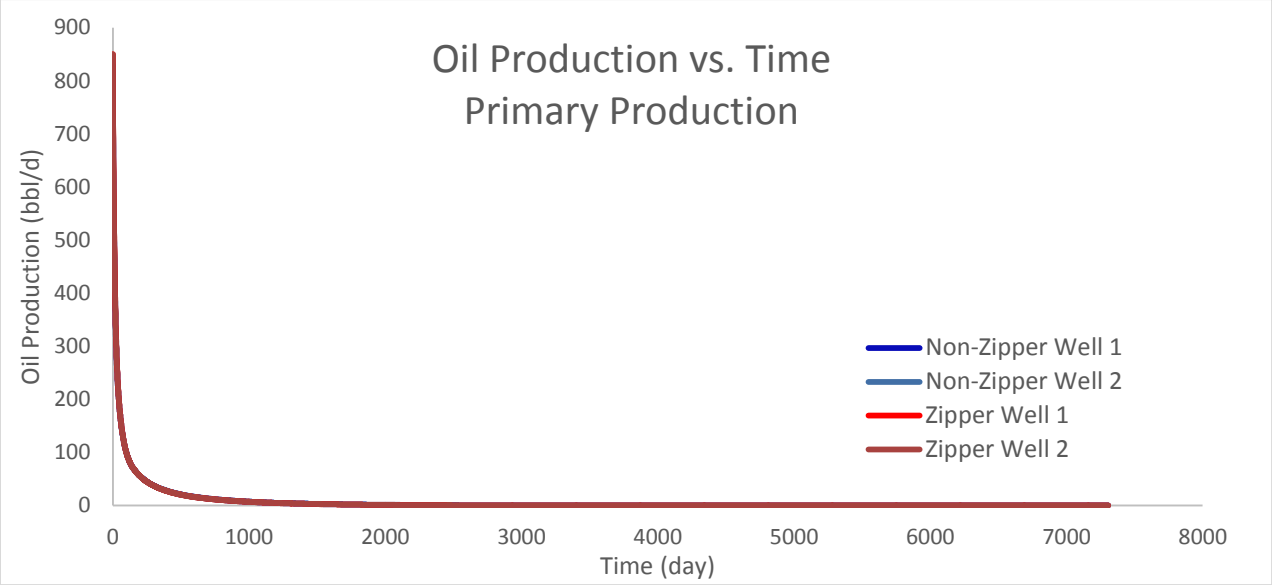

Figure 4.3: Primary Oil Productions for 20 Years.

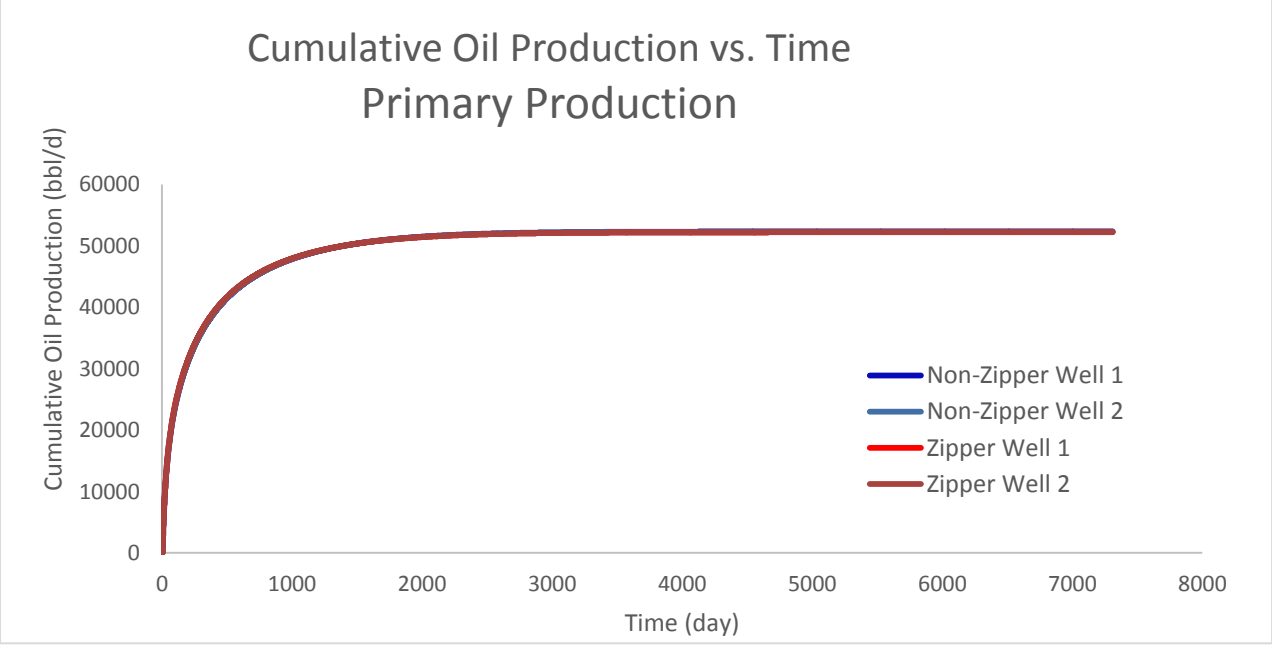

Figure 4.4: Primary Cumulative Oil Production for 20 Years.

Same relation is carried to cumulative oil production data for a year production. Cumulative oil production for zipper and non-zipper hydraulic fracture cases compromises for 20 years production for exact same reservoir volume and well parameters.

4.3 CO_2 Injection

In order to increase the cumulative oil production, CO_2 injection is started after one year depletion. For both cases, same reservoir portions which are used on depletion will be used for CO_2 injection (Chapter 3). One of the wells will turn into injection well after a year production for both cases and the other well will remain as producer well all times. CO_2 injection will continue for 9 years and then production will continue for 10 years. CO_2 injection cases will be compared with 20 year depletion cases as well as the two different hydraulic fracture configurations.

Different cyclic injection and soak times and different injection rates are tested. Table 4.2 summarizes different scenarios applied for both zipper and non-zipper hydraulic fractured cases.

Table 4.2: CO_2 Injection Scenarios

CO_2 Cyclic Injection With Different Injection and Soak Times				CO_2 Cyclic Injection With Different Injection Rates	
Cases	Injection Time (day)	Soak Time (day)	Production Time (day)	Cases	Injection Rate (MMSCF/D)
Base Case	15	15	15	Base Case	5
Case A	10	20	30	Case D	10
Case B	20	10	30	Case E	20
Case C	30	30	30	Case F	50

Figure 4.5 and Figure 4.6 show oil production and cumulative oil production for different CO_2 cyclic injection time periods. In all cases the recoveries increase with very similar trends. Although the results do not quite change from each other, the greatest values are gained with Case C which is 30 day of injection, 30 day of soak and 30 day of production and the least is gained by Case B 20 day of injection, 10 day of soak and 30 day of production. This is because the greatest soak time is in Case C. When comparing Base Case which is 15 day of injection, 15 day of soak and 30 day of production and Case A which is 10 day of injection, 20 day of soak and 30 day of production, Case A gives slightly better results. Again Case A has higher duration time than Base case. Also for non-zipper and zipper hydraulic fracture cases the results for each case are parallel to each other and zipper hydraulic fracture case. For depletion, non-zipper and zipper hydraulic fracture cases have only 82 bbl difference. The recoveries are always slightly higher for zipper hydraulic fracture case for CO_2 injection, around 1000 bbl for 20 years. The highest improvement with CO_2 injection is 17,927 bbl for zipper hydraulic fracture orientation in Case C. The results are tabulated and shown in Table 4.3.

Table 4.3: CO_2 Cyclic Injections with Different Injection and Soak Times

Cases	Total CO_2 Injection (MMSCF)	Total Injection Duration (day)	Cumulative Oil After 20 Year (BBL)		Improvement With CO_2 (BBL)	
			Zipper	Non-Zipper	Zipper	Non-Zipper
Depletion	-	-	52411	52329	-	-
Base Case	4050	810	67093	65996	14682	13667
Case A	5400	1080	67320	66507	14909	14178
Case B	2700	540	66077	65285	13666	12956
Case C	5400	1080	70338	69173	17927	16844

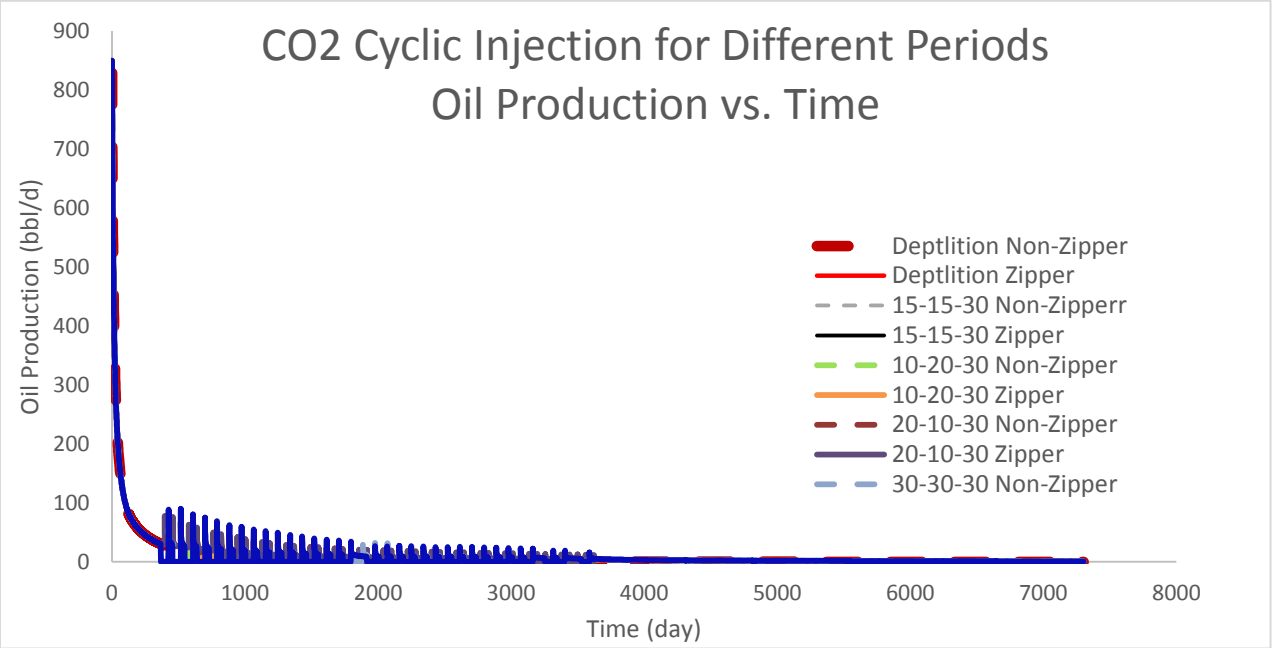

Figure 4.5: Oil Production for 9 Year CO_2 Cyclic Injection for Different Time Periods.

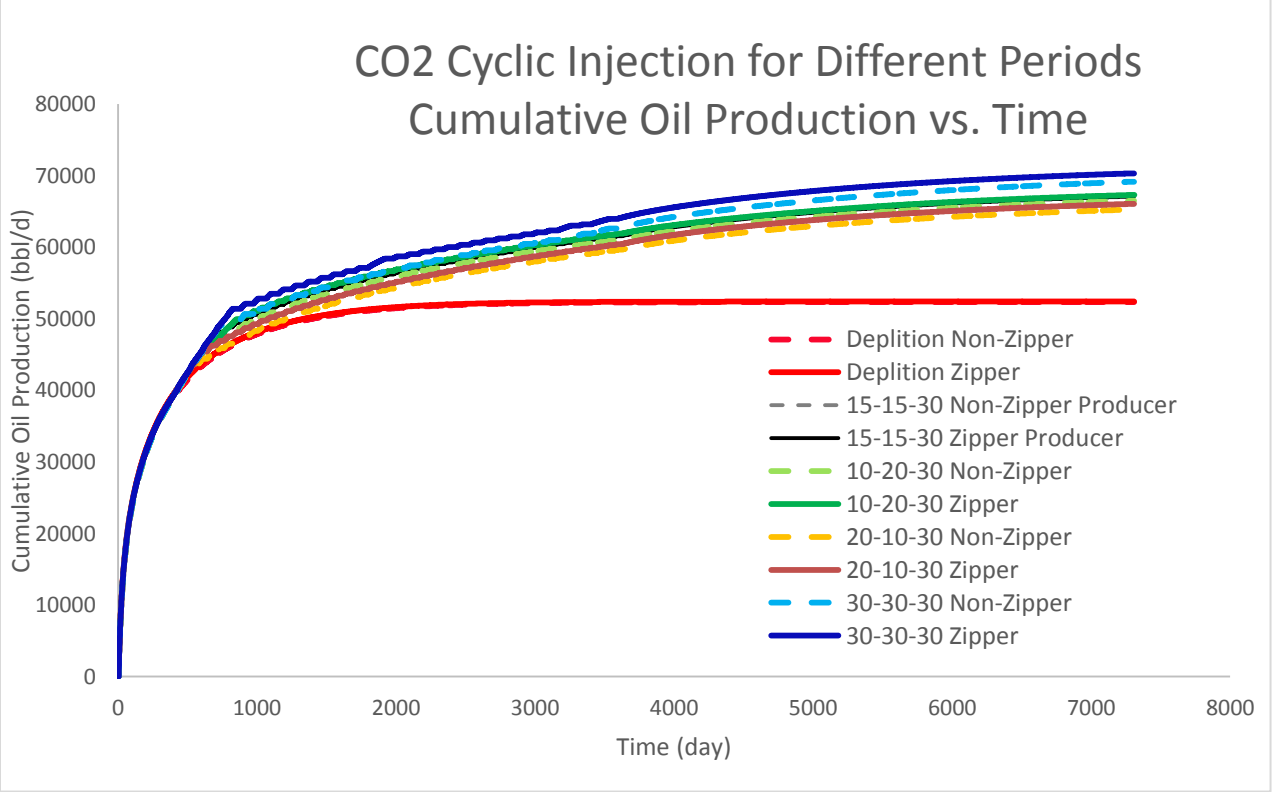

Figure 4.6: Cum. Oil Production for 9 Year CO_2 Cyclic Injection for Different Times.

Figure 4.7 and Figure 4.8 shows oil production and cumulative oil production for different CO_2 cyclic injection rates. In all cases the injection time, duration and production are equal to Base Case which is 15 day of injection, 15 day of soak and 30 day of production. The recovery performances increase with increasing CO_2 injection rate. Similar to different cyclic time periods cases, the recoveries increases with very similar trends. And the zipper hydraulic fracture case has better recovery factor for all cases and it also increases with increasing CO_2 injection rate. The difference in improvement for non-zipper and zipper hydraulic fracture cases starts with 1015 barrel for Base Case which has 5 MMSCF/D injection rate and reaches to 2563 bbl for Case F which has 50 MMSCF/D injection rate . With higher CO_2 injection rates, the performance of the zipper hydraulic fracture case can be observed better. The results are tabulated and shown in Table 4.4.

Table 4.4: CO_2 Cyclic Injections with Different Injection Rates

Cases	Total CO_2 Injection (MMSCF)	Total Injection Duration (day)	Cumulative Oil After 20 Year (BBL)		Improvement With CO_2 (BBL)	
			Zipper	Non-Zipper	Zipper	Non-Zipper
Depletion	-	-	52411	52329	-	-
Base Case	4050	810	67093	65996	14682	13667
Case D	8100	810	69022	67592	16677	15263
Case E	16200	810	70146	68033	17735	15704
Case F	40500	810	71771	69125	19359	16796

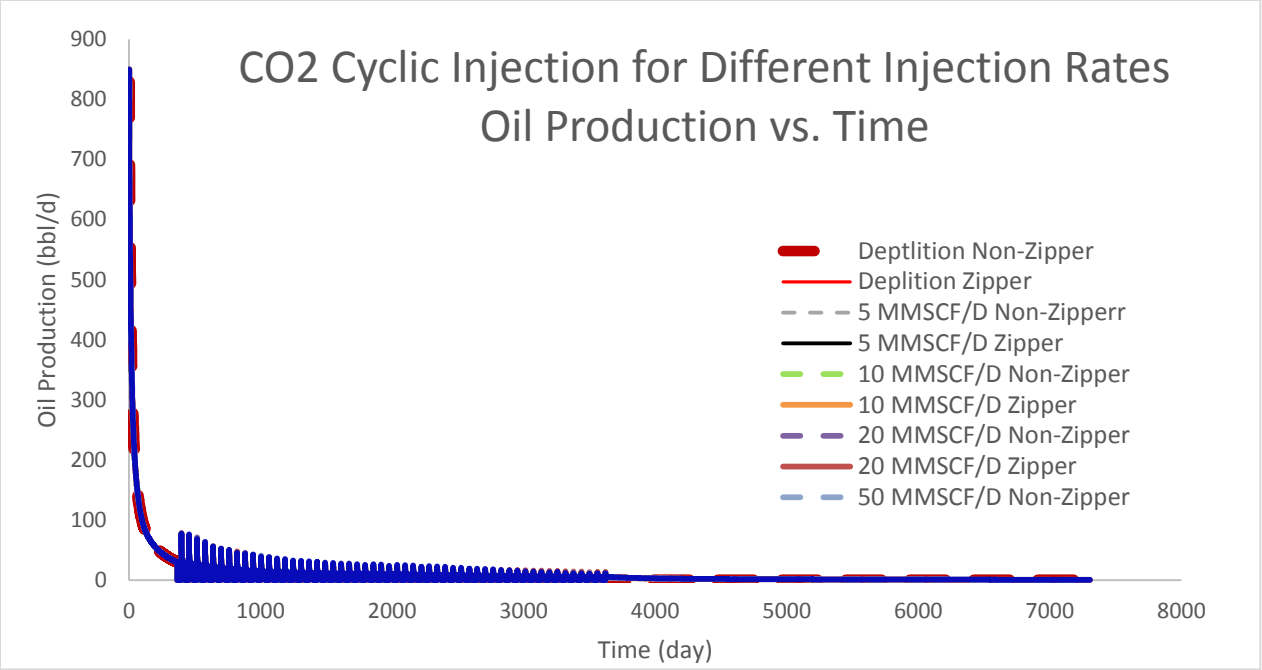

Figure 4.7: Oil Production for 9 Year CO_2 Cyclic Injection for Different Injection Rates.

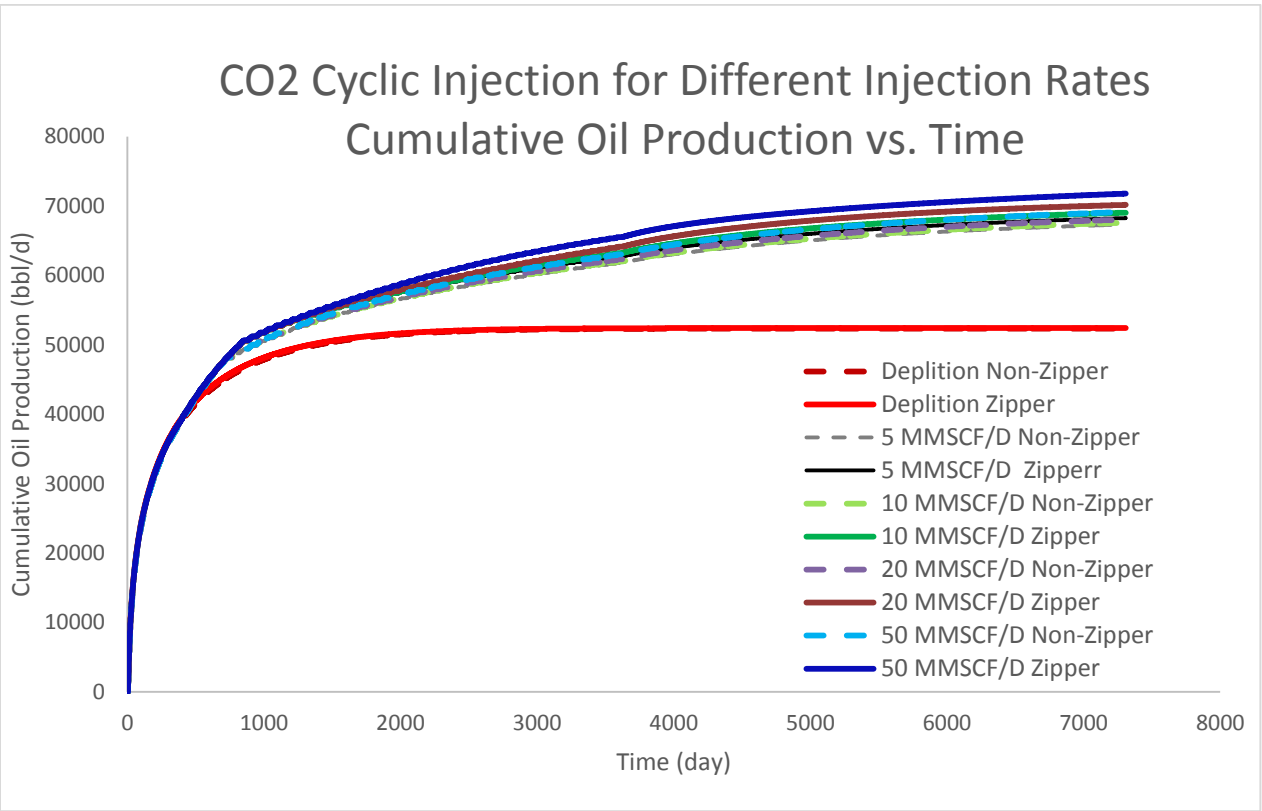

Figure 4.8: Cum. Oil Production for CO_2 Cyclic Injection for Different Injection Rates.

All of the cases which have been compared do not include a diffusion coefficient in the model which means that the only flow driving CO_2 to penetrate the reservoir matrix is advective flow which will not enable CO_2 to enter microscopic scale pores. Here the molecules can only enter in the tight matrix one by one instead of entering in as bulk volume (Whitson and Brule, 2000). In order to enter into matrix which has very low permeability and contains the main oil, diffusion takes place which occurs in molecular level. Molecular diffusion is the main mechanism to mix oil and CO_2 in sense of multi-contact miscibility, which the common assumption, by reaching local equilibrium is based for numerical simulation of CO_2 flooding in pore scale (Renner, 1988). To account for diffusive flow, diffusion coefficient is added to the model and the results are compared with depletion and base case. Table 4.5 summarizes the compared models with diffusion coefficient.

Table 4.5: Diffusion Coefficient Comparison Case

CO_2 Cyclic Injection	
Cases	Diffusion Coefficient (cm^2/s)
Depletion	-
Base Case	-
Case G	10^{-2}

The result are plotted to compare the difference with diffusion coefficient and shown in Figure 4.9 and Figure 4.10.

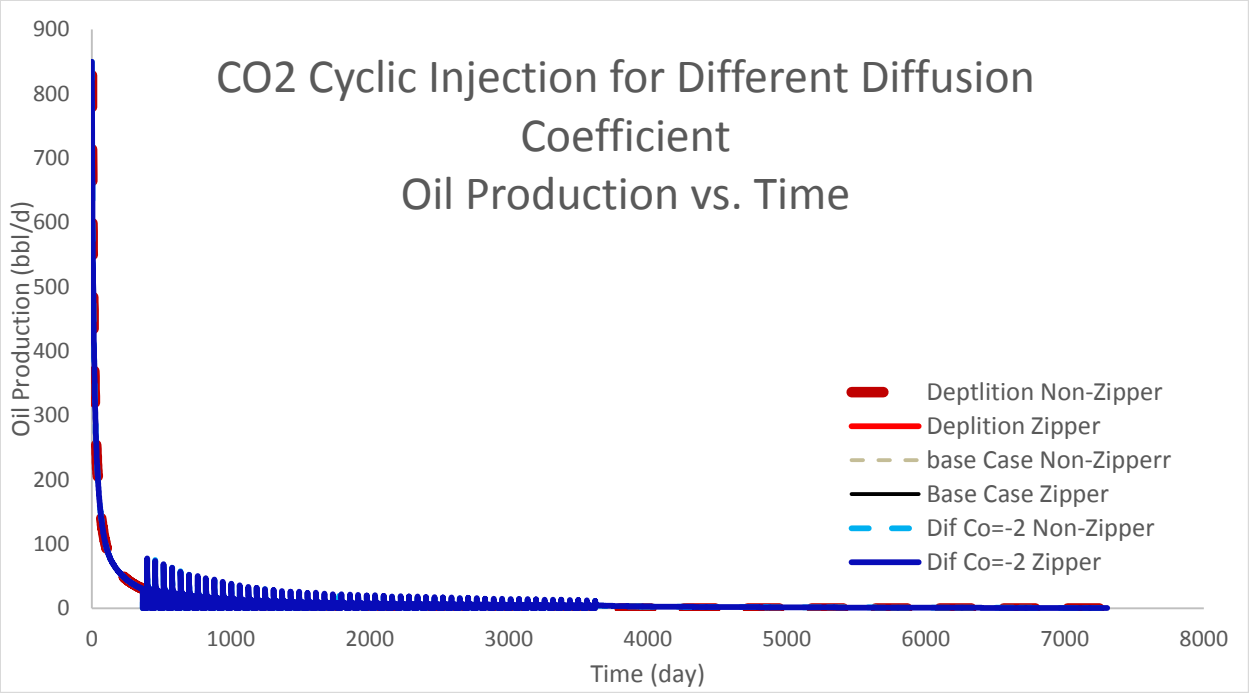

Figure 4.9: Oil Production for 9 Year CO_2 Cyclic Injection with Diffusion Coefficient.

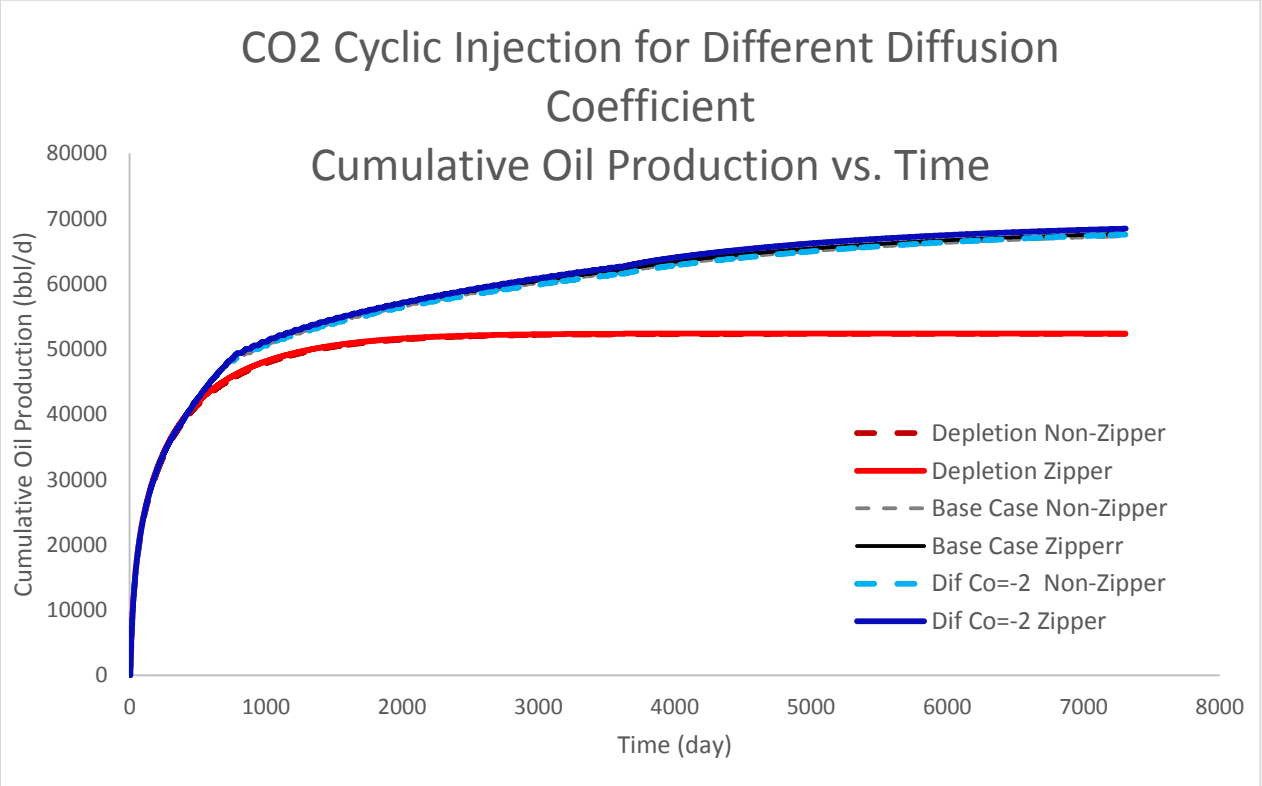

Figure 4.10: Cum. Oil Production for CO_2 Cyclic Injection with Diffusion Coefficient.

From the graphs, the effect of the diffusion coefficient may be observed. From the cumulative oil production, total cumulative oil production is enhanced but not significant enough. Even though the diffusion coefficient chosen, 10^{-2} cm^2/s, is a high value for oil-CO_2 systems, the effect is not notable. The results are tabulated and shown in Table 4.6.

Table 4.6: Diffusion Coefficient Comparison

Cases	Diffusion Coefficient (cm^2/s)	Total CO_2 Injection (MMSCF)	Total Injection Duration (day)	Cumulative Oil After 20 Year (BBL)		Improvement With CO_2 (BBL)	
				Zipper	Non-Zipper	Zipper	Non-Zipper
Depletion	-	-	-	52411	52329	-	-
Base Case	-	4050	810	67093	65996	14682	13667
Case G	10^{-2}	4050	810	68472	67561	16061	15232

From the results, the improvement is 1500 barrel better for Case G than Base Case. The differences between non-zipper and zipper hydraulic fracture cases are around 1000 barrel for both cases.

CHAPTER 5

CONCLUSIONS

A dual-porosity, fully compositional model was developed for a hypothetical Bakken reservoir to determine the performance of zipper hydraulic fracture pattern compared to a non-zipper hydraulic fracture pattern both for primary production and CO_2 injection. The following are the conclusions.

Main Conclusion:

- Overall, we did not observe much improvement in oil recovery using the zipper fracture pattern versus a regular fracture pattern when the reservoir properties are identical. However, we expect that zipper fracture to have a better permeability than a geometrically equivalent non-zipper fracture, which should lead the zipper fracture to have better performance.

Detailed Conclusions:

- In primary production, zipper and non-zipper hydraulic fractures perform essentially the same.
- For CO_2 EOR, cyclic injection was used. The base case consisted of 15 days of injection at 5 MMSCF per day of CO_2, 15 days of soak, and 30 days of production). The zipper fracture performed slightly better than non-zipper case.
- Higher CO_2 injection rates produced higher recoveries.
- The molecular diffusion effect was insignificant even with values as large as 10^{-2} cm^2/s.

NOMENCLATURE

Unit of Measurement Abbreviations

BBL : barrel

cp : centipoise

D : day

ft : feet

F : Fahrenheit temperature

md : millidarcy

psi : pound per square inch

RB : reservoir barrel

STB : stock tank barrel

Symbols

B : formation volume factor, L^3/L^3 (RB/STB)

c_t : total reservoir compressibility, L^2F^{-1} (1/psi)

h : formation thickness, L (ft)

$k_{f,eff}$: effective fracture permeability, L^2 (md)

k_{rg} : gas relative permeability in liquid-gas system, (fraction)

k_{rog} : oil relative permeability in liquid-gas system, (fraction)

k_{row} : oil relative permeability in water-oil system, (fraction)

k_{rw} : water relative permeability, (fraction)

k_{rg} * : oil relative permeability end-point , (fraction)

k_{rog} * : oil relative permeability end-point in liquid-gas system, (fraction)

k_{row} * : oil relative permeability end-point in water-oil system, (fraction)

k_{rw} * : water relative permeability end-point , (fraction)

m_l : slope of linear flow, $FL^{-2}t^{-1/2}$ (psi/hr$^{1/2}$)

n_{hf} : total number of fractures

n_g : Corey exponent for gas

n_{og} : Corey exponent for oil in liquid-gas system

n_{ow} : Corey exponent for oil in water-oil system

n_w : Corey exponent for water

q_t : total production rate, L^3t^{-1} (BBL/D)

P_{wf} : flowing bottom-hole pressure, FL^{-2} (psi)

S_g : gas saturation, (fraction)

S_{gr} : Irreducible gas saturation, (fraction)

S_{kf} : apparent skin

S_l : liquid saturation, (fraction)

S_{lr} : Irreducible liquid saturation, (fraction)

S_o : oil saturation, (fraction)

S_{or} : Irreducible oil saturation, (fraction)

S_w : water saturation, (fraction)

S_{wr} : Irreducible water saturation, (fraction)

t : time (D)

y_{hf} : fracture half-length, L (ft)

Greek

λ_t : total mobility, L^3t/m (md/cp)

ϕ : porosity, fraction

REFERENCES

DuBose, K., 2012, Bakken Shale Play, <http://bakkenshale.com> Accessed March 14, 2015.

Eker, I., Kurtoglu, B., and Kazemi, H., 2014. Multiphase Rate Transient Analysis in Unconventional Reservoirs: Theory and Applications Society of Petroleum Engineers SPE-171657.

Energy Information Administration (EIA), 2013. Technically Recoverable Shale Oil and Shale Gas Resources: An Assessment of 137 Shale Formations in 41 Countries Outside the United States.

Gaswirth, S. B., 2013, Assessment of Undiscovered Oil Resources in the Bakken and Three Forks Formations, Williston Basin Province, Montana, North Dakota, and South Dakota, 2013: USGS National Assessment of Oil and Gas Fact Sheet 2013-3013, 4 p.

Gaswirth, S.B., Marra, K.R., Cook, T.A, Charpentier, R.R., Gautier, D.L., Higley, D.K., Klett, T.R., Lewan, M.D., Lillis, P.G., Schenk, C.J., Tennyson, M.E., and Whidden, K.J., 2013, Assessment of undiscovered oil resources in the Bakken and Three Forks Formations, Williston Basin Province, Montana, North Dakota, and South Dakota, 2013: U.S. Geological Survey Fact Sheet 2013–3013, 4 p., http://pubs.usgs.gov/fs/2013/3013/.

GEM® Reservoir Simulating Software Version 2012.20: Computer Modelling Group.

Jarrell, P. M., Fox, C. E., Stein, M. H., and Webb, S. L., 2002. Practical Aspects of CO_2 Flooding, Vol. 22, Richardson, Texas: Monograph Series, SPE.

Kazemi, H., Merrill, L. S., Porterfield, K. L., and Zeman, P. R., 1976. Numerical Simulation of Water-Oil Flow in Naturally Fractured Reservoirs. Society of Petroleum Engineers. doi:10.2118/5719-PA.

Kazemi, H., Vestal, C. R., and Shank, D., 1978. An Efficient Multicomponent Numerical Simulator. SPE Journal, 18(5), 355-368. SPE 6890-PA. http://dx.doi.org/10.2118/6890-PA

Kurtoglu, B., 2013. Integrated Reservoir Characterization and Modeling in Support on Enhanced Oil Recovery. PhD Dissertation, November 2013, Petroleum Engineering, Colorado School of Mines, USA.

Kurtoglu. B. and Kazemi. H., 2012. Evaluation of Bakken Performance Using Coreflooding, Well Testing, and Reservoir Simulation. Paper SPE 155655 Presented in SPE Annual Technical Conference and Exhibition, 8-10 October 2012, San Antonio, Texas, USA.

LeFever, J. A., and LeFever, R. D., 2005, Salts in the Williston basin, North Dakota: North Dakota Geological Survey Report of Investigations No. 103, 45 p.

Meissner, F.F. 1978. Petroleum geology of the Bakken Formation Williston Basin, North Dakota and Montana, 1978 Williston Basin Symposium: Billings, Montana, Montana Geological Society, p. 207–227.

North Dakota Geological Survey, Industrial Commission (NDIC), 2015. Director's Cut, North Dakota monthly oil production statistics website https://www.dmr.nd.gov/oilgas/stats/historicaloilprodstats.pdf, Accessed April 17, 2015.

Pilcher, R.S., Ciosek, J.M., McArthur, K., Holman, J., and Schmitz, P.J., 2010. Ranking Production Potential Based on Key Geological Drives-Bakken Case Study. Paper IPTC 14773, International Petroleum Technology Conference, Bangkok, Thailand, February 7-9.

Pitman, J.K., Price, L.C., and LeFever, J.A. 2001. Diagenesis and Fracture Development in the Bakken Formation, Williston Basin: Implications for Reservoir Quality in the Middle Member. U.S. Geological Survey Professional Paper 1653.

Price, L.C. 1999. Origins and Characteristics of the Basin-Centered Continuous Reservoir Unconventional Oil-Resource Base of the Bakken Source System, Williston Basin: Unpublished manuscript, http://www.undeerc.org/Price/, Accessed 24 March 2015.

Rafiee, M., Soliman, M.Y., and Pirayesh. E. 2012. Hydraulic Fracture Design and Optimization: A Modification to Zipper Frac. Society of Petroleum Engineers. SPE-159786-MS http://dx.doi.org/10.2118/159786-MS.

Renner, T. A. 1988. Measurement and Correlations of Diffusion Coefficients in Reservoir Fluids. SPE Res. Eng. 3:517-523.

Shoaib, S. and Hoffman, B.T., 2009. CO_2 Flooding the Elm Coulee Field. Paper SPE 123176 presented at the SPE Rocky Mountain Petroleum Technology Conference held in Denver, Colorado, USA, 14-16 April 2009.

Sonnenberg, S.A. and Pramudito, A., 2009. Petroleum Geology of the Giant Elm Coulee Field, Williston Basin. AAPG Bulletin, V.93, No.9 (September, 2009), PP.1127-1153.

Stone, H. L., 1973, Estimation of Three-Phase Relative Permeability and Residual Oil Data, Can.Pet.Tech., Vol 12, Page 53-61.

Teklu, T. W., Alharthy, N., Kazemi, H., Yin, X., Graves, R. M., and AlSumaiti, A. M. (2014, August 1). Phase Behavior and Minimum Miscibility Pressure in Nanopores. Society of Petroleum Engineers. doi:10.2118/168865-PA.

Theloy, C., and Sonnenberg, S. A. (2013, August 12). Integrating Geology and Engineering: Implications for Production in the Bakken Play, Williston Basin. Society of Petroleum Engineers. doi:10.1190/URTEC2013-100.

USGS Release. 2008. 3 to 4.3 Billions Barrels of Technically Recoverable Oil Assessed in North Dakota and Montana's Bakken Formation- 25 Times More Than 1995 Estimate, available from http://www.usgs.gov/newsroom. Accessed 10 April 2008.

User Guide GEM. 2012. CMG Compositional Reservoir Simulator.

Wang, X., Luo, P., E., V., and Huang, S., 2010. Assessment of CO2 Flooding Potential for Bakken Formation, Saskatchewan. Paper CSUG/SPE 137728 presented at the Canadian

Unconventional Resources & International Petroleum Conference, Calgary, Alberta, Canada, 19-21 October 2010.

Warpinski, N.R., Mayerhofer, M.J., Vincent, M.C., Cipolla, C.L., and Lolon, E.P. 2009. Stimulating Unconventional reservoirs: Maximizing Network Growth While optimizing Fracture Conductivity. Journal of Canadian Petroleum Technology (10): 39-51.

Waters, G.A., Dean, B.K., Downie, R.C., Kerrihard, K.J., Austbo, L., and McPherson, B., 2009. Simultaneous Hydraulic Fracturing of Adjacent Horizontal Wells in the Woodford Shale. SPE paper 119635-MS presented at the SPE Hydraulic Fracturing Technology Conference, Woodlands, Texas, 19-21 January.

Webster, R.L. 1984. Petroleum Source Rocks and Stratigraphy of the Bakken Formation in North Dakota, in J. Woodward, F. F. Meissner, and J. C. Clayton, eds., Hydrocarbon Source Rocks of the Greater Rocky Mountain Region: Denver, Rocky Mountain Association of Geologists, p. 57–81.

Whitson, C.H. and Brule, M.R. 2000. Phase Behavior. SPE Monograph V.20.

WINPROP® Reservoir Simulating Software Version 2012.20: Computer Modelling Group.